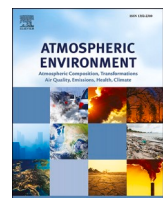




ELSEVIER

Contents lists available at ScienceDirect

Atmospheric Environment

journal homepage: <http://www.elsevier.com/locate/atmosenv>

Evaluation of real-time PM_{2.5} forecasts with the WRF-CMAQ modeling system and weather-pattern-dependent bias-adjusted PM_{2.5} forecasts in Taiwan

Fang-Yi Cheng ^{a,*}, Chih-Yung Feng ^b, Zhih-Min Yang ^b, Chia-Hua Hsu ^{a,c}, Ka-Wa Chan ^a, Chia-Ying Lee ^a, Shuenn-Chin Chang ^d

^a Department of Atmospheric Sciences, National Central University, Taiwan

^b Manysplendid Infotech, Taipei, Taiwan

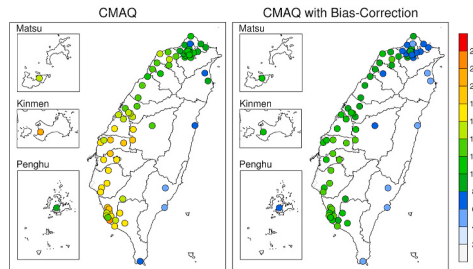
^c Department of Mechanical Engineering, University of Colorado, Boulder, CO, USA

^d Environmental Protection Administration, Taipei, Taiwan

HIGHLIGHTS

- Development of an air quality forecasting system using WRF-CMAQ model framework.
- Assessment of one-year PM_{2.5} forecasts indicate a consistent under-prediction.
- Variation of synoptic weather pattern has a significant impact on PM_{2.5} problem.
- Apply a bias-correction method that accounts for the synoptic weather patterns.
- The bias-correction method effectively reduces the PM_{2.5} forecasting bias.

GRAPHICAL ABSTRACT



ARTICLE INFO

Keywords:

Air quality forecasting system
PM_{2.5} forecast
Bias correction
Synoptic weather pattern
WRF-CMAQ

ABSTRACT

A real-time air quality forecasting (AQF) system was developed in Taiwan using the Weather Research and Forecasting meteorological model and Community Multiscale Air Quality model framework. This study evaluated the performance of the one-year archived AQF PM_{2.5} forecasts (October 2018 to September 2019) and developed a bias-correction method to improve the accuracy of the PM_{2.5} forecasts.

The bias-correction method incorporates a cluster-analysis-based synoptic weather pattern (WP) classification (one type of analog method). In principle, the historical model errors are categorized according to the synoptic WP and used to adjust the PM_{2.5} forecast. First, the synoptic WPs are determined using K-means cluster analysis (six WPs were identified). Second, the historical AQF PM_{2.5} bias at each surface station is estimated for each classified WP. Third, a linear-regression relationship between the AQF PM_{2.5} bias and PM_{2.5} forecasts for the six WPs is developed to postprocess the PM_{2.5} forecasts.

The AQF PM_{2.5} bias is found to have a strong dependency on the synoptic WP. A performance assessment of the AQF PM_{2.5} forecasts reveals systematic PM_{2.5} underprediction, with the most pronounced underprediction occurring on days associated with weak synoptic weather conditions. Under these conditions, a severe PM_{2.5} event is likely to occur in Taiwan. The bias-correction method is able to reduce the PM_{2.5} forecast error and improve the root mean square error (RMSE) and mean bias (MB) calculations. The improvement is most

* Corresponding author.

E-mail address: bonniecheng18@gmail.com (F.-Y. Cheng).

significant on days associated with a weak synoptic WP and in regions where high PM_{2.5} concentrations are likely to occur. The method is shown to be effective at reducing the AQF PM_{2.5} bias.

1. Introduction

Fine particulate matter (PM_{2.5}), especially its role in severe haze events, has become a significant public concern in Taiwan. From autumn to the next spring season, the prevailing northeasterly (NE) to easterly wind (depending on the location of the Asian continental anticyclone system) is obstructed by the Central Mountain Range (with peaks as high as 3952 m), and low wind speeds and strong subsidence occur over the leeside of the mountains, often leading to high PM_{2.5} accumulation and causing severe PM_{2.5} events in western Taiwan (Hsu and Cheng, 2019). It is important to provide accurate PM_{2.5} forecasts to administrative agencies and the general public in advance to prevent exposure to high PM_{2.5} levels.

Chemical transport models (CTMs) have been widely used to provide daily air quality forecasts (Ghim et al., 2017; Lee et al., 2017; Mathur et al., 2008; Otte et al., 2005; Žabkar et al., 2015). To meet the public demand for immediate information on PM_{2.5} forecasts, a real-time air quality forecasting (AQF) system using the Weather Research and Forecasting (WRF) meteorological model version 3.8.1 (Skamarock et al., 2008) and Community Multiscale Air Quality (CMAQ) model version 5.2 (Byun and Schere, 2006; Byun and Ching, 1999) was developed in Taiwan in July 2015. Since then, various efforts have been made to improve its forecasting performance (Lin and Chen, 2016; Cheng and Chen, 2018; Cheng et al., 2019; Hsu et al., 2019). Despite these efforts, substantial prediction errors remain because of uncertainties in emission inventories and meteorological forecasts, as well as the incomplete physical and chemical mechanisms in the CTMs.

Emission inventory uncertainties include the inadequate estimation of anthropogenic emission sources, incorrect use of emission factors, lack of the most up-to-date emission information, and inaccurate temporal allocation of emission sources (Holnicki and Nahorski, 2015; Hsu et al., 2019; Zhao et al., 2011). Moreover, the biogenic emission estimates vary significantly due to variations in plant species and uncertainties in the estimation methodologies. Meteorological forecasting errors arise from an imperfect initial state, inaccurate lower boundary conditions, approximated physical parameterizations, and relatively coarse horizontal resolution that is unable to resolve small spatial and temporal scales (Cheng et al., 2013; Gilliam et al., 2015; McNider and Pour-Bazar, 2020). The Central Mountain Range of Taiwan runs from north to south across the entire island, which further complicates meteorological simulations in Taiwan (Cheng et al., 2012, 2019; Lai and Lin, 2020).

Although prediction errors remain in the modeling system, they are not completely random; in fact, these errors tend to exhibit a systematically biased pattern, which could be attributed to missing or incorrect emission sources or systematic meteorological errors. To improve the daily AQF capability, bias-correction techniques are typically applied to adjust model forecasts and remove systematic errors. Various bias-correction methods have been proposed to postprocess the model outputs (e.g., Gómez-Navarro et al., 2018; Huang et al., 2017; Kang et al., 2010a, b). In principle, these methods incorporate historical model errors to adjust the current model forecasts. The Kalman filter (KF) has been widely used to correct future forecasts from a model's historical biases (De Ridder et al., 2012; Delle Monache et al., 2006). Kang et al. (2008) applied KF adjustment techniques to improve ozone (O₃) forecasting. The method is effective at reducing biases at low but not high O₃ concentrations because high O₃ levels occur less frequently and the 12-km model grid is often unable to simulate the peak O₃ levels.

Another commonly used bias-correction method is the analog method, which classifies historical forecasts into similar analogs. Then, historical analog bias is used to correct future model bias (Delle

Monache et al., 2014; Lyu et al., 2017). Huang et al. (2017) utilized an analog ensemble bias-correction approach to improve experimental PM_{2.5} predictions over the contiguous United States. They used the PM_{2.5}, 2-m temperature and 10-m wind fields to find the similarity between current and historical forecasts and corrected the future forecasts with the historical analog forecast bias. Other studies combined the analog method with the KF method to determine the ensemble bias within the same analog. Djalalova et al. (2015) applied different post-processing techniques, including a running mean subtraction, the KF, analogs, and combinations of analogs and the KF, to correct the PM_{2.5} predictions from the National Oceanic and Atmospheric Administration (NOAA) developmental AQF (stajner et al., 2012) and indicated that a KF method applied to historical analogs has the best forecast skill for PM_{2.5}.

In this study, we propose a bias-correction method for PM_{2.5} predictions to account for synoptic weather pattern (WP) classifications using the K-means approach. In principle, it is assumed that pollutant levels have a strong response to weather conditions and circulation patterns. According to Hsu and Cheng (2019), air pollutant concentrations are strongly affected by synoptic weather systems, the prevailing wind field, and local circulation. For example, when the northeasterly monsoonal (NEM) flow prevails in Taiwan, the long-range-transported air pollutants from other countries in East Asia can affect the local air quality in Taiwan. The predicted PM_{2.5} bias can be attributed to the uncertainties in the East Asia emissions inventory or errors associated with the meteorological conditions, such as an inaccurate simulation of the NEM flow. On the other hand, if the synoptic flow weakens, the reduced dispersion can result in the accumulation of local emissions and cause elevated air pollution concentrations. Under this circumstance, the predicted PM_{2.5} bias is mainly the result of uncertainties in the Taiwan emissions inventory or errors in the predicted local air flow, such as the land-sea breeze circulation. Previous modeling studies have indicated that the WRF model tends to overestimate the onshore sea-breeze flow along the coastal area of western Taiwan, which leads to an underestimation of the simulated PM_{2.5} and its precursors (Chen et al., 2013; Hsu et al., 2019). It is rational to assume that the bias characteristics are related to the synoptic WPs.

WPs or circulation pattern-based bias-correction methods have been used in climate model simulations to correct rainfall distributions (Bárdossy and Pegram, 2011; Photiadou et al., 2016). Li et al. (2018) proposed a synoptic pattern-based bias correction using self-organizing map classification (Kohonen, 2001) and obtained results that were significantly different from those of a conventional quartile mapping method.

The goals of this study are outlined as follows: (1) evaluate the performance of the AQF system-predicted PM_{2.5} concentrations in Taiwan; (2) develop a bias-correction method that incorporates several synoptic WPs and circulation types; and (3) examine the performance of the proposed bias-correction method. Section 2 describes the AQF system, the classified synoptic WPs, the bias-correction method, and the experimental designs. The performance of the raw model PM_{2.5} forecasts and the impact of the bias-correction method are presented in Section 3. Further discussions of the bias-correction method and of its applicability in the real-time AQF system in the future and the conclusions are given in Sections 4 and 5. To the best of our knowledge, this is the first study conducted in Taiwan that evaluates the performance of PM_{2.5} forecasts from the CTM-based framework and assesses the performance of the bias-correction methodology. Lee et al. (2020) used a machine learning technique to predict the PM_{2.5} concentrations in Taiwan, and the evaluation revealed a reliable 24-h prediction at most air quality stations.

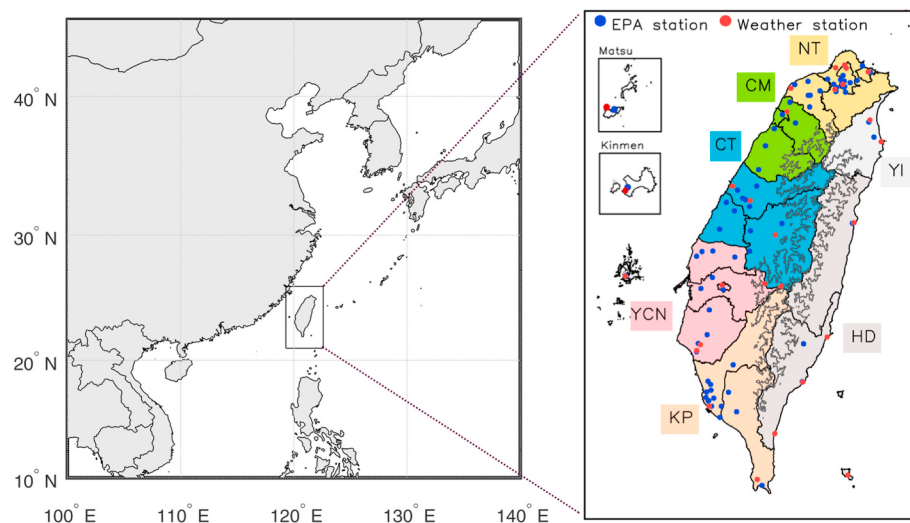


Fig. 1. The left panel shows the AQF system modeling domains. The right panel displays the locations of the surface air quality monitoring stations and surface weather stations. Seven subregions (NT, CM, CT, YCN, KP, YI and HD) and off-island stations are identified. The contour line indicates the Central Mountain Range.

Table 1
CMAQ model configurations.

Chemical mechanism	Carbon Bond (CB05) (Yarwood et al., 2005)
Aerosol module	Aerosol module version six (AERO6) (Appel et al., 2017)
Advection scheme	Yamartino advection (YAMO)
Horizontal diffusion	Multiscale (Byun et al., 1999)
Vertical diffusion	Asymmetric Convection Model (Pleim, 2007)

2. Methodology and experimental design

2.1. Taiwan AQF system

The real-time AQF system has been under operation in Taiwan since July 2015 and contains three major components. First, the WRF meteorological model, version 3.8.1, provides hourly meteorological fields to drive the CTM. The initial and boundary conditions are obtained from the Global Forecast System (GFS) weather forecast model on 0.25-degree grids produced by the National Centers for Environmental Prediction (NCEP). Second, the US EPA's CMAQ model, version 5.2, which simulates transport, chemistry and deposition processes, provides spatial and temporal PM_{2.5} predictions. The WRF-CMAQ system is applied in an offline paradigm. A two-level nested domain is employed (Fig. 1), with a spatial resolution of 15 km for the coarse domain (D1), which encompasses East Asia, and a spatial resolution of 3 km for the fine domain (D2), which covers the Taiwan region. Third, an emission processing system provides the anthropogenic emissions in D1 from the 2010 Model Inter-Comparison Study for Asia (MICS-Asia) emissions inventory (Li et al., 2017) and the anthropogenic emissions in D2 from the Taiwan Emission Data System, version 9.0 (TEDS-9.0, 2013), for which the base year is 2013. Biogenic emissions are provided by the Model Of Emissions Of Gases And Aerosols From Nature (MEGAN) (Guenther et al., 2012). The initial conditions for all domains are from the CMAQ forecasting output of the previous day, and the boundary conditions of D1 are based on the default background profile datasets, which are static and does not change with the time. The boundary conditions for D2 are provided by D1. The physical and chemical configurations of the CMAQ model are listed in Table 1.

In this study, the year-long archived PM_{2.5} forecasts from October 2018 to September 2019 were evaluated against the observed surface dataset to understand the performance of the AQF system-predicted PM_{2.5} concentrations in Taiwan and to examine the performance of the proposed bias-correction method.

2.2. Observation datasets

The hourly PM_{2.5} concentrations from the Taiwan Environmental Protection Administration (TWEPA) surface air monitoring stations were used for model validation. In total, 77 monitoring stations were available to verify the model's performance (refer to Fig. 1 for site locations).

Due to the distinct characteristics of the meteorological and emission conditions, the TWEPA has divided the nation into seven subregions, namely, northern Taiwan (NT), the Chu-Miao area (CM), central Taiwan (CT), the Yun-Chia-Nan area (YCN), the Kao-Ping area (KP), the Yilan (YI) and the Hua-Dong area (HD) (Fig. 1). The subsequent evaluation and discussion are organized based on these seven subregions plus one off-island subregion to facilitate the performance verification. There are three off-island stations, of which Matsu and Kinmen are located less than 10 km from the coast of China.

2.3. Synoptic weather pattern classification

We developed a bias-correction technique that incorporates a cluster analysis-based classification of synoptic WPs (considered one type of analog method). The first step was to identify the synoptic WPs. Following a previous study (Hsu and Cheng, 2019), a two-stage clustering method was applied to classify the synoptic WPs. The daily averaged values of the hourly U and V wind speeds and the sea level pressure (SLP) at the surface weather stations in Taiwan (refer to Fig. 1 for station locations) were used for cluster analysis. In the first stage, a hierarchical method was used to determine the initial number of clusters and the centroids of the clusters. To be consistent with the finding of Hsu and Cheng (2019), six clusters were used, and the centroids of each cluster were determined based on Hsu and Cheng (2019), for which the surface U, V and SLP data from January 2013 to March 2018 were used for WP classification.

In the second stage, the centroids of the six clusters were used as seeds for the initiation of the K-means cluster analysis (MacQueen, 1967). The daily synoptic WP of the one-year study period (October 2018 to September 2019) was classified using K-means cluster analysis. Details of the classification method can be found in Hsu and Cheng (2019). We excluded the days affected by a tropical depression (TD) or typhoon because their low occurrence frequency lacks statistical representativeness. During the one-year study period, there were 9 days affected by a TD or typhoon weather system. Those days were excluded from the analysis and evaluations conducted in this study. After the

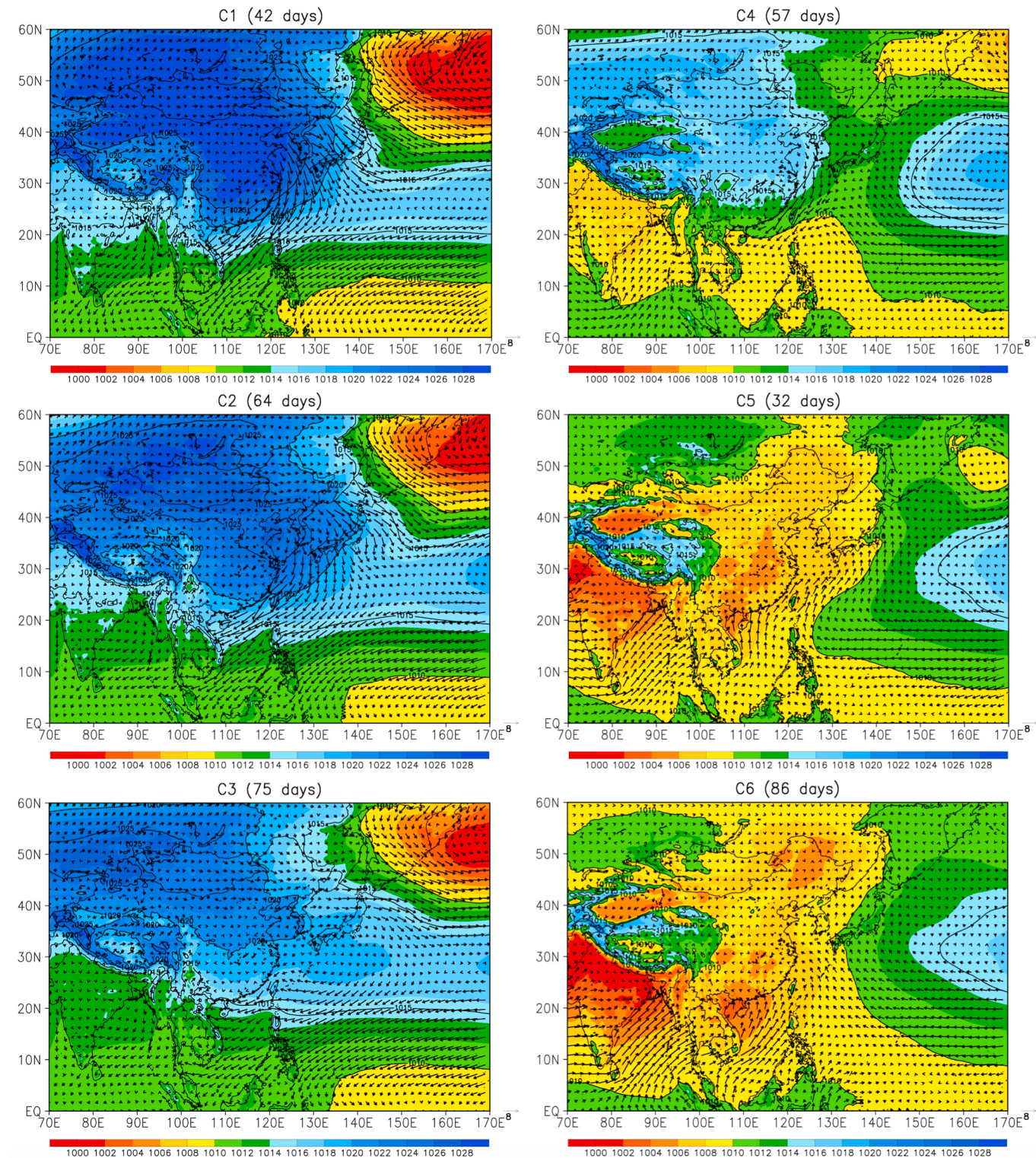


Fig. 2. Composite plots of sea level pressure (hPa) (shaded colors) and surface wind vectors (m s^{-1}) for the six WPs. The number of days that occurred in each cluster is identified. (For interpretation of the references to color in this figure legend, the reader is referred to the Web version of this article.)

cluster analysis, six synoptic WPs types were identified in the area of Taiwan.

Fig. 2 shows composite maps of the mean SLP and wind fields of the six WPs from the ERA5 reanalysis data (Hersbach and Dee, 2016) for the one-year study period (October 2018 to September 2019). For cluster 1 (C1), the prevailing wind in Taiwan is dominated by the NEM flow due to the intrusion of the Asian continental anticyclone. For cluster 2 (C2),

with the eastward movement of the Asian continental anticyclone, the prevailing wind in Taiwan is affected by weak northeasterly to easterly flows due to continental high-pressure peripheral circulation. When the continental anticyclone is located farther away from the Asian continent, Taiwan is under the influence of weak synoptic weather (cluster 3, C3) and affected by a weak easterly to southeasterly flow. Cluster 4 (C4) mainly occurs during the seasonal transition months, with a weak NEM

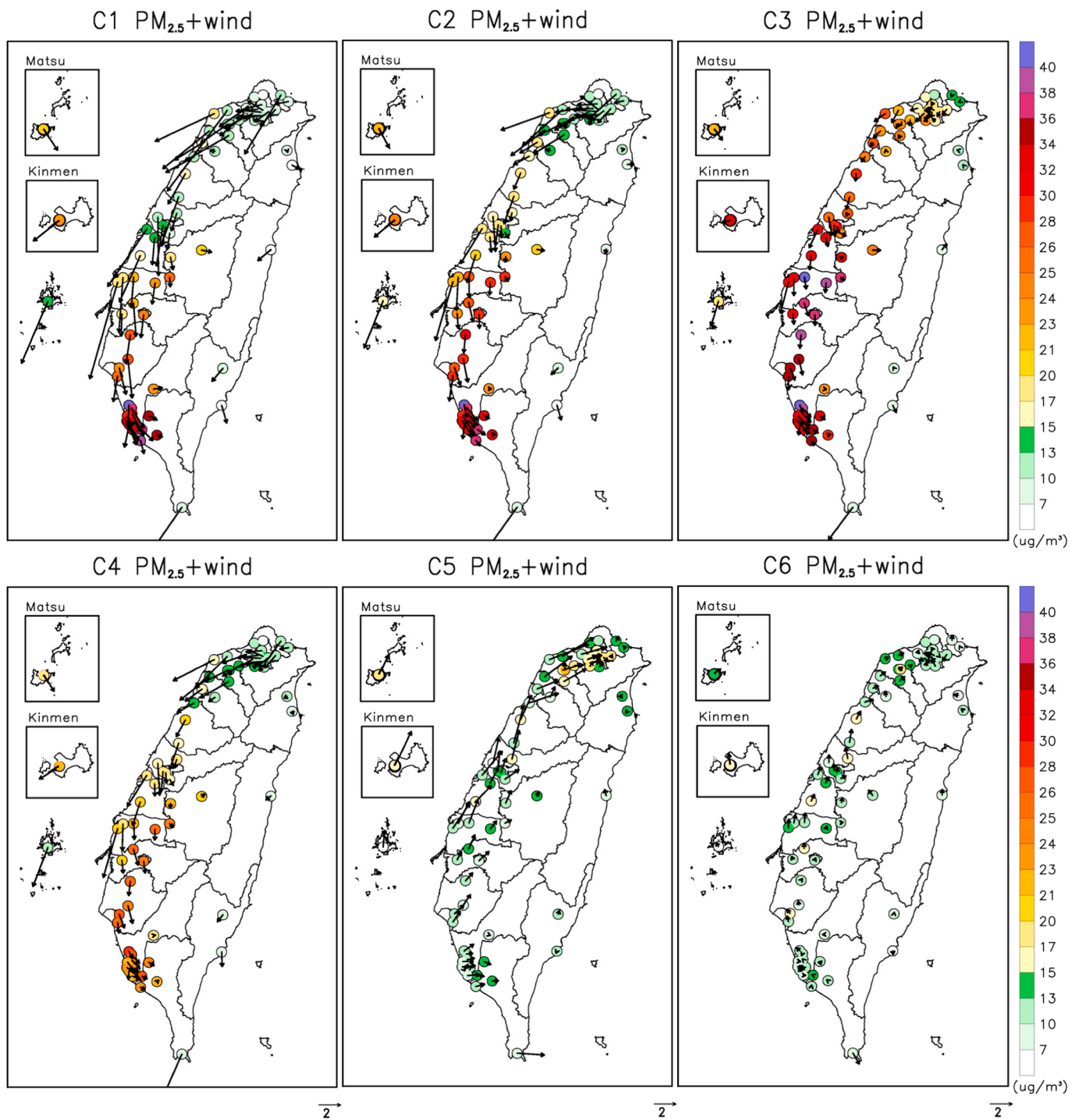


Fig. 3. Distributions of the daily mean PM_{2.5} concentrations ($\mu\text{g}/\text{m}^3$) and wind vectors (m/s) from the TWEPA surface stations for each cluster.

flow prevailing in Taiwan. The WP of cluster 5 (C5) is dominated by westward stretching of the subtropical high-pressure system. For cluster 6 (C6), the influence of the subtropical high-pressure system is weaker than that for C5, and the prevailing wind in Taiwan is mainly affected by a southwesterly flow.

Fig. 3 shows the distributions of the daily mean PM_{2.5} concentrations and wind vectors observed at the TWEPA surface stations and averaged over the days that occurred in each weather type. C1 is associated with the strongest wind fields due to the influence of the East Asian winter monsoon system. Clusters C1–C3 mainly occur during the autumn, winter and spring seasons and are associated with higher PM_{2.5} concentrations than the other clusters. The highest PM_{2.5} concentrations

occur in southwestern Taiwan due to stagnant wind conditions and emissions from multiple sources transported from the upwind and surrounding areas (Hsu and Cheng, 2019). C4 mainly appears during the seasonal transition months with slightly lower PM_{2.5} concentrations than the C1–C3 clusters. C5 and C6 mainly occur in the summer and have low PM_{2.5} concentrations. The prevailing southerly wind in the C5 cluster can sometimes result in an accumulation of PM_{2.5} in northern Taiwan if under the influence of stable synoptic weather conditions. Among the six WPs, the worst PM_{2.5} problem occurs in the C3 cluster. Due to the weak influence of the synoptic weather system, as western Taiwan is situated on the leeside of the mountain, this area has stagnant wind conditions, which leads to PM_{2.5} accumulation in C3. The YCN

Table 2

Number of days, mean PM_{2.5} ($\mu\text{g m}^{-3}$) concentrations, wind speed (WS) (m s^{-1}), and daily accumulated precipitation (mm) averaged over Taiwan for each cluster.

	Number of days	PM _{2.5}	WS	Rainfall amount
C1	42	17.43	2.86	2.43
C2	64	19.46	2.10	2.21
C3	75	25.44	1.54	1.58
C4	57	17.13	2.09	5.05
C5	32	12.84	1.95	3.69
C6	86	11.70	1.60	14.89

subregion in C3 suffers from the most severe PM_{2.5} pollution.

Table 2 summarizes the occurrence days, mean PM_{2.5} concentrations, wind speed, and daily accumulated rainfall averaged for the TWEPA surface stations in Taiwan for each cluster from October 2018 to September 2019. The lowest wind speed and the highest PM_{2.5} concentrations are observed in C3. C5 and C6 are summer-related WPs and are associated with low PM_{2.5} concentrations. The highest rainfall amount occurs in C6 and is mainly induced by afternoon thunderstorms. The results of the WP analysis are consistent with the findings from Hsu and Cheng (2019) and do not vary significantly when data from different periods are used for WP classification, which indicates that the synoptic WP classification method developed in Hsu and Cheng (2019) is a reliable technique and can be applied for any extended data periods in the future.

2.4. Bias-correction method and experimental designs

First, the hourly biases are estimated using the historical AQF PM_{2.5} forecasts and observations at individual monitors and are categorized according to the six synoptic WPs. The bias-correction method is applied at only the locations of the monitors. Next, a linear-regression relationship ($y = ax + b$) is established for the individual WPs for each forecast hour and at each station, assuming that the PM_{2.5} bias (y) varies linearly with the PM_{2.5} forecast (x). Parameters a and b are calibrated using the WP-categorized training datasets. If the linearity assumption of the regression model does not pass the statistical t -test (null hypothesis is accepted with the significance level of 0.05), the linear-regression model is not used for bias correction. Instead, the average PM_{2.5} forecast bias at each station and each hour is directly applied (running mean subtraction). This method is named the WP-based bias-correction (WP-BC) method. **Fig. 4** illustrates the percentages of the running mean subtraction and linear-regression model applied in correcting the one-year CMAQ PM_{2.5} forecasts (October 2018 to September 2019) for each WP. The linear-regression model approach is more likely to be selected in clusters C1 to C5 during most hours of the day, while the running mean subtraction approach is the preferred method in cluster C6 except during nighttime hours. Majority of the data in clusters C3 and C5 is able to pass the statistical t -test.

The scatter plot (**Fig. S1** of the supplementary material) at one surface station located in KP subregion at each hour of the C3 cluster is presented as an example to demonstrate the linear-regression relationship between PM_{2.5} bias and AQF PM_{2.5} forecast. High correlation (with correlation coefficient, $r > 0.8$) tends to be seen from hour 00 to 09 LST while the correlation degrades ($0.3 < r < 0.8$) during hours 10 to 23 LST. **Table S1** of the supplementary material further summarizes the correlation coefficients between the PM_{2.5} biases and the AQF PM_{2.5} forecasts averaged from the TWEPA surface stations for each cluster at each hour. The correlation coefficient is between 0.4 and 0.8, indicating a moderate positive correlation. **Fig. S1** and **Table S1** only considers the data that pass the statistical t -test.

Hsu and Cheng (2019) indicated that high PM_{2.5} events frequently occur due to the reduced atmospheric ventilation capability and unfavorable meteorological conditions from autumn to the next spring season, when the synoptic weather conditions are dominated by the East

Asian winter monsoon. On the other hand, several studies have indicated that the strength of the East Asian winter monsoon has weakened due to global warming (Hori and Ueda, 2006). Cheng and Hsu (2019) mentioned that the reduced strength of the East Asian winter monsoon decreases the atmospheric dispersion capability, which in turn worsens the local air pollution. The bias of the AQF system can be affected by changes in the East Asian winter monsoon system. Moreover, recently, there has been a substantial reduction in Taiwan anthropogenic emissions due to enforced control strategies, such as reductions in power plants emissions, replacement of old diesel cars, and replacement of coal burning boilers with cleaner natural gas-fired boilers. Variations in emissions, together with synoptic circulation patterns, can complicate the statistical representativeness of bias patterns. In this study, the year-long evaluation period from October 2018 to September 2019 is used to limit the variability in anthropogenic emissions and East Asian winter monsoons. Moreover, a consistent configuration of the AQF system was in effect from October 2018 to September 2019.

The AQF PM_{2.5} forecasts are divided into two datasets, with one dataset for calibration and the other for validation. Validations are conducted day by day. For example, October 1, 2018, is classified as C4 WP, and to validate the hourly PM_{2.5} forecasts on this day, the calibration dataset consists of the remaining 56 days in the C4 cluster (excluding the data for the validation date, e.g., October 1, 2018). The calibration dataset is considered to be a training dataset and is used to derive the coefficients, which are applied in the linear-regression equation to correct the validation dataset.

The evaluation of the one-year archived PM_{2.5} forecasts provides a general understanding of the ability of the WP-BC method to correct the CMAQ PM_{2.5} forecasts. One of the deficiencies in the one-year evaluation is that the information from the future is used to correct the PM_{2.5} bias, which limits the applicability of the WP-BC method in real-time AQF systems because future information would not be available in operational systems. As a result, an additional experiment was conducted using the data from the one-year period (October 2018 to September 2019) as the training datasets, while the validation dataset targets an independent period from October 2019 to May 2020. Since June 2020, the AQF operational system has experienced a major change in anthropogenic emissions; therefore, the second experiment does not extend beyond June 2020. The purpose of the second experiment is to investigate the feasibility of applying the WP-BC method in the real-time AQF system in the future. A complete assessment of the one-year evaluation from October 2018 to September 2019 is presented in the following section, while the evaluation results of the second experiment are discussed in Section 4.

3. Assessment of the AQF PM_{2.5} forecasts and WP-dependent bias-correction method

3.1. Evaluation of year-long AQF PM_{2.5} forecasts

The 3-km grid spacing CMAQ PM_{2.5} forecasts are evaluated against the surface air quality monitoring stations. **Figs. 5 and 6** present the mean bias (MB) of the CMAQ PM_{2.5} forecasts from October 2018 to September 2019 at the surface stations associated with six WPs. The MB evaluations are separated into daytime (0800–1900) (**Fig. 5**) and nighttime (2000–0700) (**Fig. 6**) hours.

The PM_{2.5} biases of the off-island stations behave similarly in both daytime and nighttime conditions and lead to systematic underprediction. However, over Taiwan Island, the PM_{2.5} bias behaves differently between daytime and nighttime conditions. The bias in eastern Taiwan (YI and HD subregions) is lower than that in the other subregions.

For the daytime comparisons, there is systematic PM_{2.5} underprediction for all the WPs at all the air quality monitoring stations except some stations located in NT and CT. The underprediction is more apparent in central extending to southwestern Taiwan than in northern

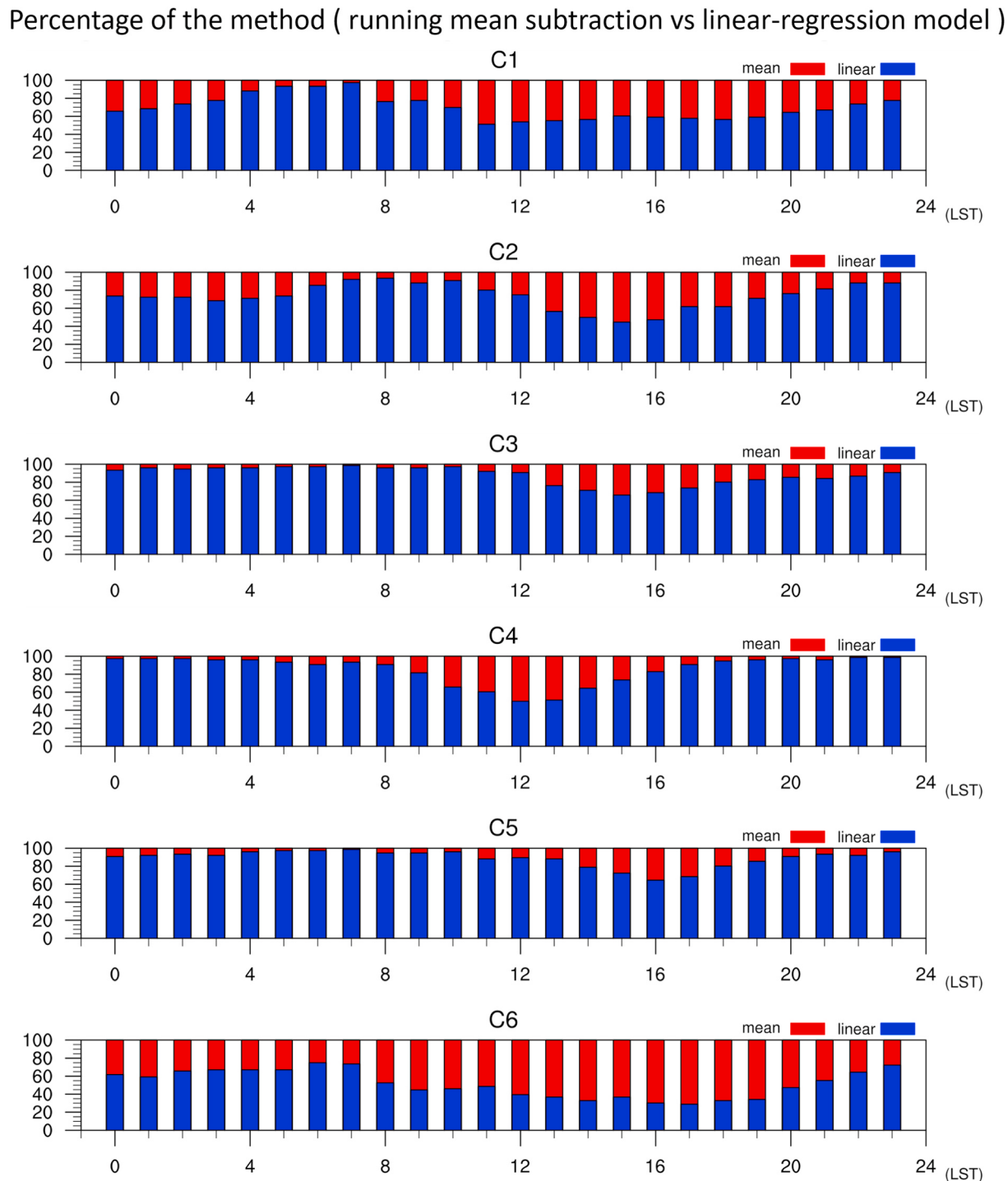


Fig. 4. Percentages of the running mean subtraction and linear-regression model applied in the correction of the one-year CMAQ PM_{2.5} forecasts (October 2018 to September 2019) for each WP.

Taiwan. The most severe PM_{2.5} underprediction appears in the C3 cluster and occurs in the YCN subregion. Underprediction has been reported to be due to overly strong WRF-predicted wind fields (Hsu et al., 2019) and a lack of proper secondary organic aerosol (SOA) formation pathways from the CMAQ model (Murphy et al., 2017; Pye et al., 2017). In addition, the TEDS-9.0 emissions inventory does not include distant ship emissions, which are important sources of the air pollutants SO₂ and PM_{2.5}. The overly strong predicted wind fields, absence of ship emissions, uncertainty in the local emissions, and missing SOA formation pathways all contribute to the PM_{2.5} underpredictions.

For the nighttime evaluations, the bias distributions are more complex than the daytime bias distributions. Underpredictions are still seen at most surface stations; however, the magnitude is less than that under the daytime conditions. In the C1 cluster, the AQF system underpredicts the PM_{2.5} concentrations at most surface stations except northern (NT subregion) and central-western Taiwan (CT subregion). In the C2 cluster, the AQF system underpredicts in northern Taiwan but overpredicts at most stations in central to southwestern Taiwan. In the C3 cluster, overpredictions are seen in the CM, CT and KP subregions. In the C4 cluster, with the exception of the CT subregion, underpredictions are

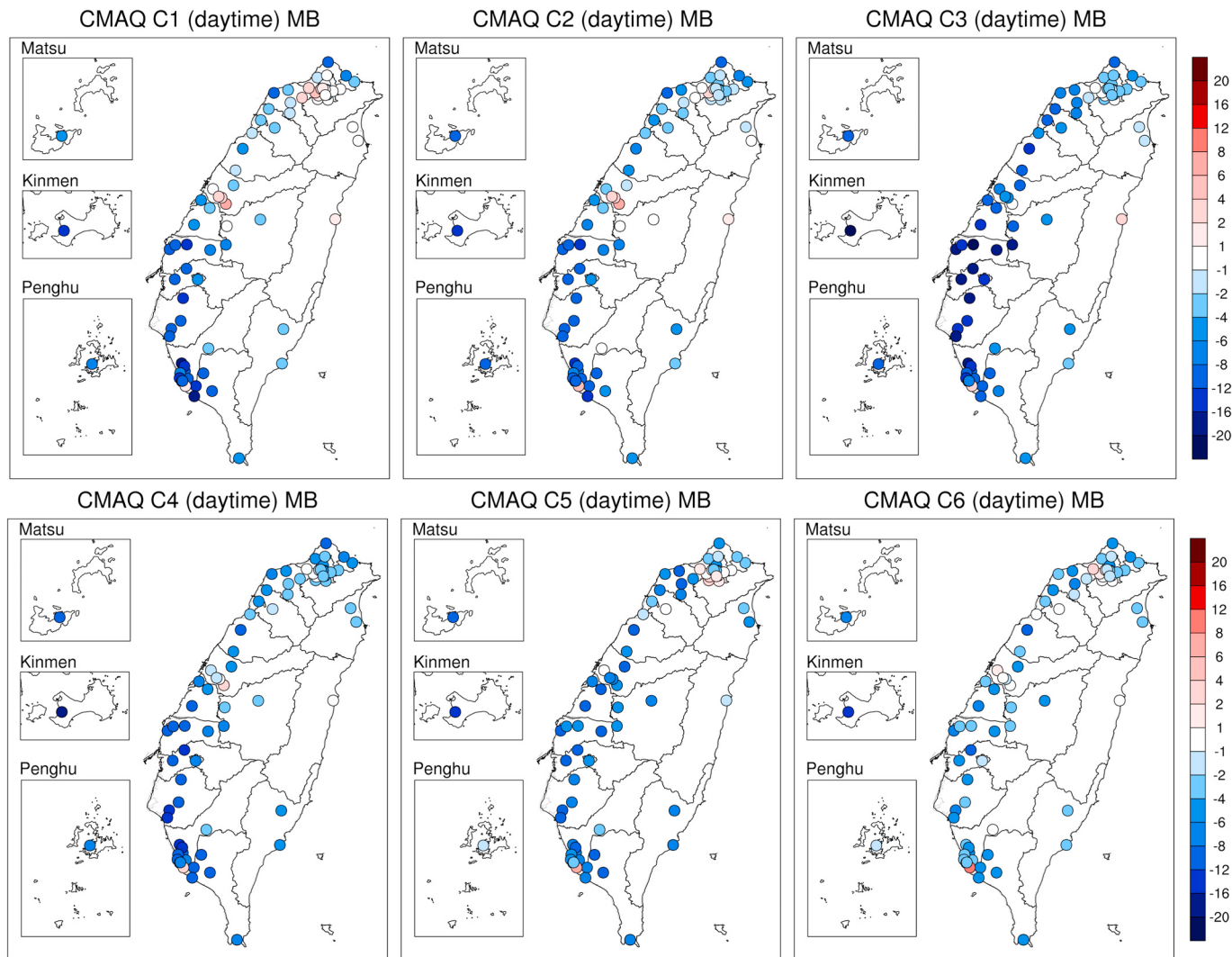


Fig. 5. MB ($\mu\text{g}/\text{m}^3$) (model minus observation value) of AQF PM_{2.5} forecasts associated with six WPs during daytime hours. Three off-island stations are shown on the left side of each figure.

seen at most stations but with a smaller magnitude than at the stations in clusters C1–C3. As discussed earlier, there is a substantial reduction in anthropogenic emissions in Taiwan due to the enforced control strategies, particularly in the CT subregion, which is not updated in the TEDS9.0 emissions inventory. The emissions inventory currently used in the AQF system overpredicts the emissions in the CT subregion and leads to PM_{2.5} overprediction there. An updated emissions inventory that reflects these replacements is greatly needed to enhance the forecasting capability. C5 and C6 are summer weather types, and their bias patterns are different from those of the C1–C4 WPs. Nighttime overpredictions are seen in northern Taiwan in the C5 cluster. Due to the prevailing southerly wind conditions, the PM_{2.5} overprediction in northern Taiwan may be due to the excessive emissions from its upwind sources. For the C6 cluster, there appears to be an overall overprediction at most stations except for the sites located in the northern tip and YCN subregion. There is significant overprediction at one station located in southwestern Taiwan for all the clusters, which is due to the site being located near the harbor and identified as a water body land-use type in the WRF modeling system. The predicted planetary boundary layer height is shallow and leads to PM_{2.5} accumulation in the AQF system.

The YCN subregion exhibits consistent PM_{2.5} underpredictions in all the clusters, and severe underprediction is seen in the C3 cluster. This underestimation can be attributed to the uncertainties in the TEDS9.0 emissions estimated for the YCN and surrounding area, to wind speed

overestimation, and to the errors in the CTMs, such as missing or incomplete SOA formation and sulfate formation pathways (Hsu et al., 2019; Zheng et al., 2015; Hung and Hoffmann, 2015). As discussed earlier, among the six WPs, C3 is the weather type associated with the highest PM_{2.5} concentrations, and the YCN subregion suffers from the worst PM_{2.5} pollution. The relative poor model performance for PM_{2.5} for the YCN subregion of the C3 cluster makes announcing national air quality alerts challenging for air quality forecasters. There is an urgent need to enhance the AQF capability, particularly over the YCN subregion.

The hourly estimation of the bias values for the six clusters is used to build the linear-regression equations for each surface station. Then, the bias-correction method is applied to correct the AQF PM_{2.5} forecasts.

3.2. Impact of the WP-BC method

Fig. 7 presents the daily mean PM_{2.5} time series averaged for the stations located in the off-island and seven subregions from observations, the AQF system, and WP-BC forecasts. The CMAQ model is able to predict the general PM_{2.5} variations, such as the accumulation or dilution behavior; however, there are apparent PM_{2.5} forecasting errors throughout the one-year evaluation period.

The off-island stations located near China present systematic PM_{2.5} underpredictions in the range of 10–20 $\mu\text{g}/\text{m}^3$, indicating that the

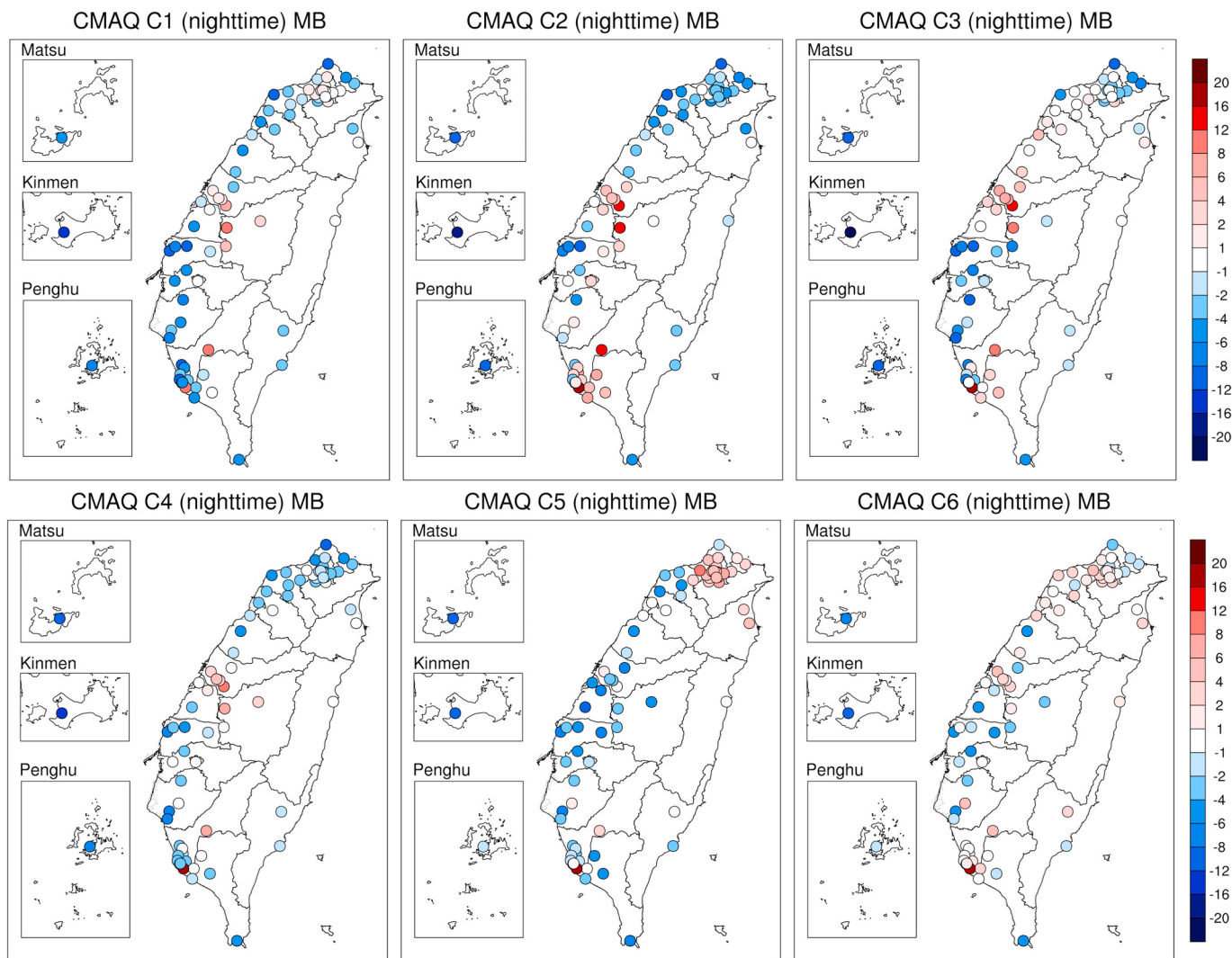


Fig. 6. MB ($\mu\text{g}/\text{m}^3$) (model minus observation value) of AQF PM_{2.5} forecasts associated with six WPs during nighttime hours. Three off-island stations are shown on the left side of each figure.

transboundary air pollutants from China may be underpredicted. The high PM_{2.5} concentrations observed at the off-island stations are mainly due to the transported PM_{2.5} from China, such as the high PM_{2.5} events occurring on January 20 and February 4–5 of 2019; however, the influence of the transboundary PM_{2.5} events in the seven local subregions of Taiwan was not apparent. Cheng and Hsu (2019) indicated that the weakened NEM flow due to regional climate change can lessen the transboundary transport of air pollutants from East Asia to Taiwan. The AQF system tends to underpredict the PM_{2.5} concentrations, while the underprediction is greatly reduced with the WP-BC method for the off-island stations. The AQF system consistently underpredicts low to moderate PM_{2.5} concentrations (10–30 $\mu\text{g}/\text{m}^3$) in all the subregions, but those biases are successfully reduced with the WP-BC method.

In the CT subregion, the AQF system predicts several high PM_{2.5} events that did not occur in reality. The WP-BC method is able to remove serious overpredictions. On the other hand, several high-PM_{2.5} events were observed in January and February of 2019 in the CT and YCN subregions; however, the AQF system and the WP-BC method cannot capture those high PM_{2.5} events. At relatively high PM_{2.5} concentrations (observed daily mean PM_{2.5} > 40 $\mu\text{g}/\text{m}^3$), the WP-BC method is not able to predict the observed peak value, which might be attributed to a linear-regression assumption used for bias correction. In the future, a nonlinear regression model can be further developed to enhance the capability of the bias-correction method.

In the YCN and KP subregion, the WP-BC method greatly enhances the PM_{2.5} forecasting capability. In the YCN subregion, on January 19, 2019, the observed high PM_{2.5} concentration was caused by extremely stable atmospheric conditions and very stagnant wind fields. The observed planetary boundary layer depth according to the Lidar observation was lower than 500 m (figure not shown). The current meteorological model still has limitations in predicting extremely stable boundary conditions due to the limitation of the boundary layer parameterization for modeling the atmospheric boundary layer (Serafin et al., 2018). For example, the often-used Monin-Obukhov surface layer similarity theory is not suitable for estimating surface fluxes under strongly stable conditions (Businger et al., 1971). Most boundary layer parameterizations have difficulty resolving nonstationary flow structures and turbulence intermittency (Holtslag et al., 2013).

There was significant underprediction on March 2, 2019. However, the WP-BC method still presented large biases due to the greater traffic emissions emitted during the long-weekend holidays, which were not included in the AQF system. The traffic flow on March 2, 2019, was 25% higher than that on the same day of the previous week (figure not shown). The biases presented on January 19 and March 2 of 2019 are considered nonsystematic errors.

The overall assessment indicates that the WP-BC method can effectively remove the systematic PM_{2.5} biases that currently exist in the AQF system, although low (<10 $\mu\text{g}/\text{m}^3$) and high (>40 $\mu\text{g}/\text{m}^3$) PM_{2.5}

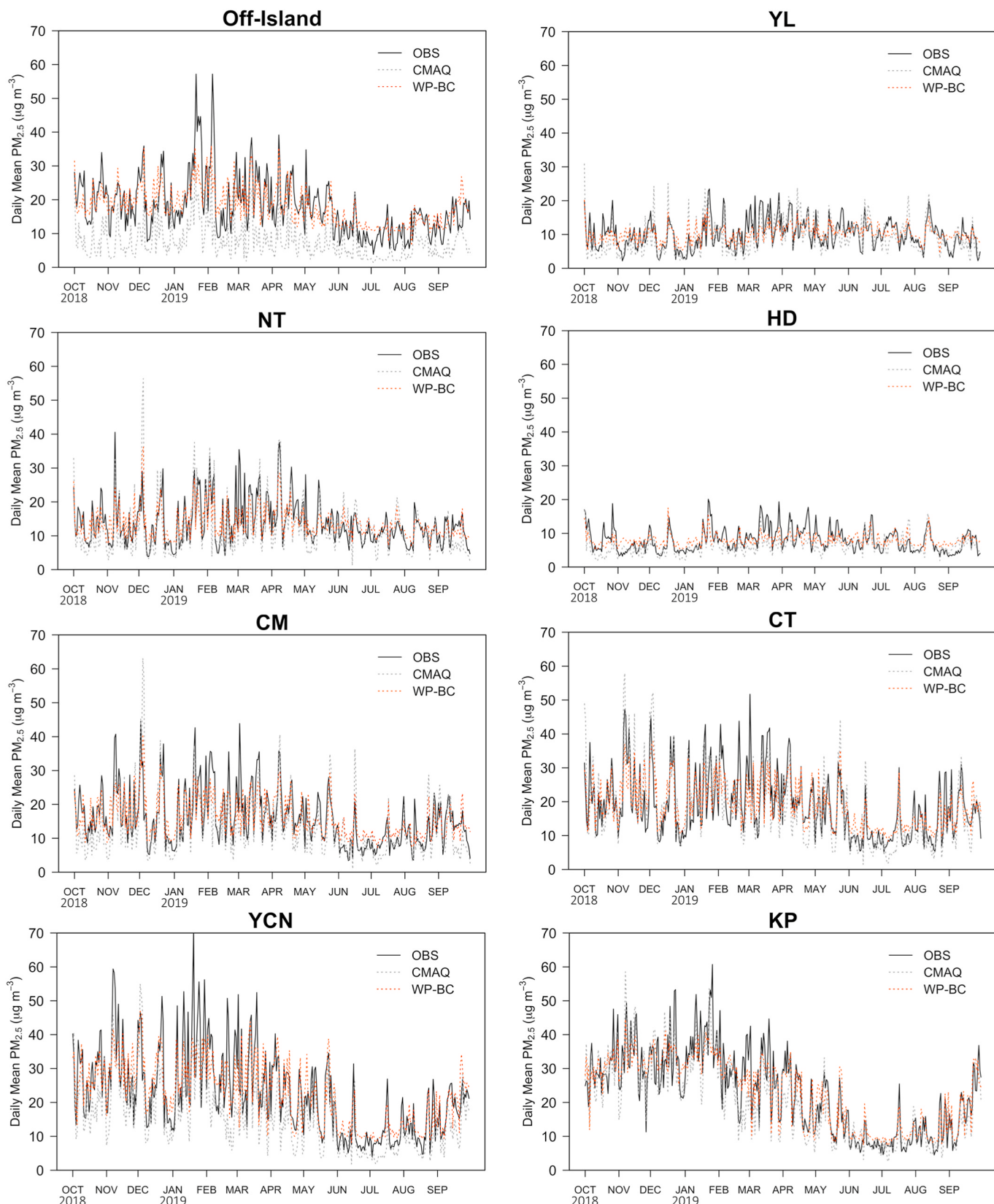


Fig. 7. Time series of daily mean $\text{PM}_{2.5}$ concentrations averaged at the surface stations located within each subregion from the observations, AQF system, and WP-BC forecast.

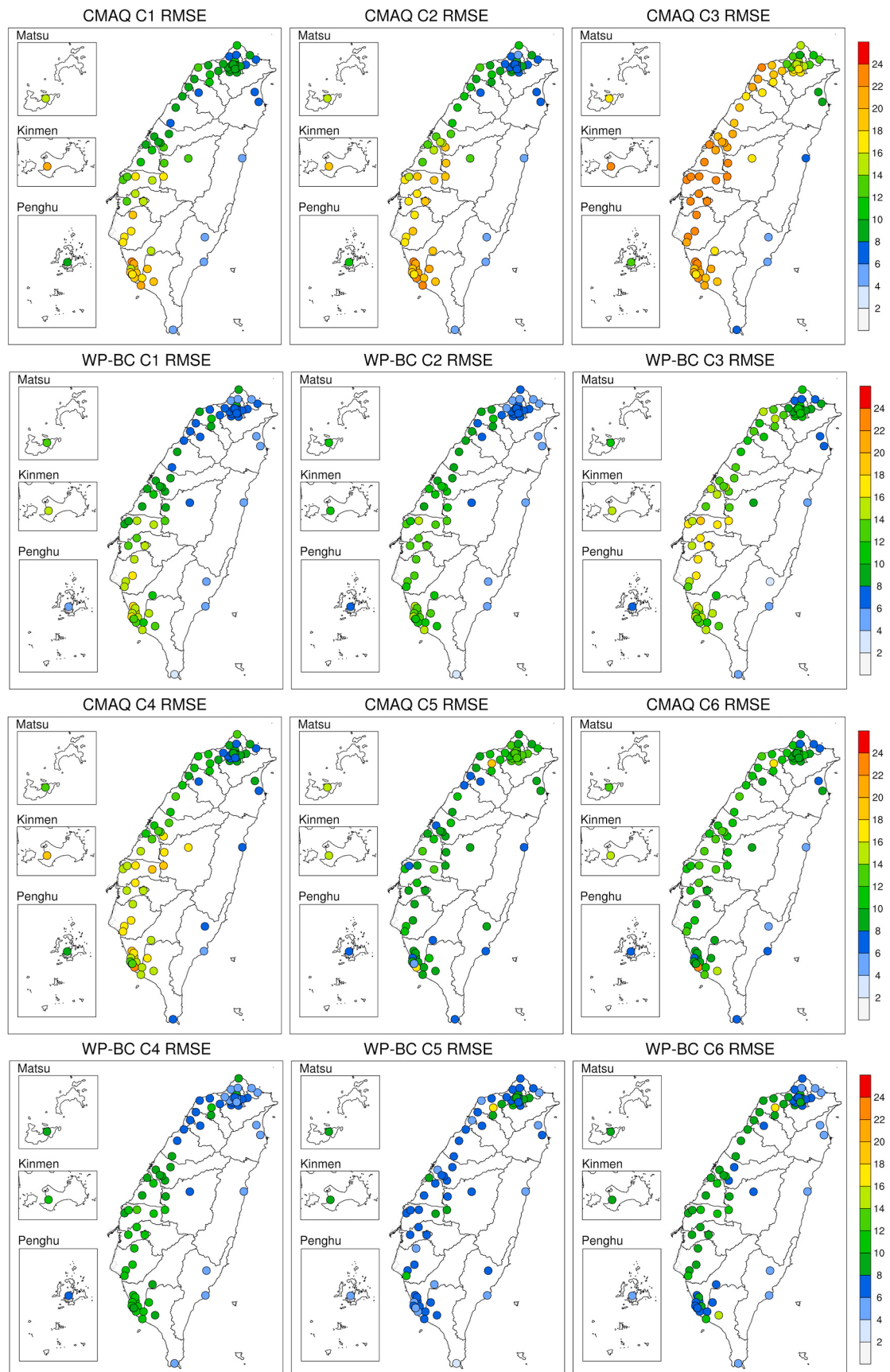


Fig. 8. RMSEs of $\text{PM}_{2.5}$ forecasts ($\mu\text{g}/\text{m}^3$) averaged from October 2018 to September 2019 at surface stations associated with six WPs. First and second row from the top is RMSEs in clusters C1 to C3 with the AQF system and WP-BC method, respectively. Third and fourth row from the top is RMSEs in clusters C4 to C6 with the AQF system and WP-BC method, respectively.

Table 3

Performance statistics for the AQF system and WP-BC daily mean PM_{2.5} forecasts from October 2018 to September 2019 in each cluster.

Cluster	N (days)	obs PM _{2.5} ($\mu\text{g}/\text{m}^3$)	PM _{2.5} forecast ($\mu\text{g}/\text{m}^3$)	M ($\mu\text{g}/\text{m}^3$)	RMSE ($\mu\text{g}/\text{m}^3$)
C1 AQF	42	17.43	14.22	-3.22	8.00
C1 WP	-	-	17.52	0.09	6.20
C2 AQF	64	19.46	16.63	-2.82	7.93
C2 WP	-	-	19.47	0.02	5.95
C3 AQF	75	25.44	21.05	-4.42	11.45
C3 WP	-	-	25.51	0.10	8.22
C4 AQF	57	17.13	13.48	-3.66	7.59
C4 WP	-	-	17.20	0.07	5.40
C5 AQF	32	12.84	10.15	-2.69	6.51
C5 WP	-	-	12.78	-0.06	4.47
C6 AQF	86	11.70	10.27	-1.42	6.10
C6 WP	-	-	11.64	-0.05	4.87

Table 4

RMSEs in seven subregions for the AQF system and WP-BC daily mean PM_{2.5} forecasts from October 2018 to September 2019 in each cluster.

Cluster	NT	CM	CT	YCN	KP	YL	HD
C1 AQF	6.07	5.58	6.87	11.23	11.27	4.04	3.84
C1 WP-BC	4.29	4.58	5.94	9.10	8.78	3.41	3.16
C2 AQF	5.73	6.19	8.38	10.24	10.36	4.80	4.22
C2 WP-BC	4.38	4.83	6.54	8.52	7.45	4.05	3.07
C3 AQF	9.67	11.82	12.30	16.27	11.34	5.34	3.96
C3 WP-BC	7.13	8.26	9.38	10.79	8.75	4.25	3.25
C4 AQF	5.68	7.01	8.53	9.95	8.96	3.93	3.86
C4 WP-BC	4.33	4.99	6.06	7.10	6.32	3.09	3.01
C5 AQF	6.19	6.11	7.01	7.06	6.26	4.14	5.13
C5 WP-BC	5.00	5.03	4.45	3.98	3.66	3.82	4.05
C6 AQF	5.59	6.68	7.01	6.52	5.88	4.32	3.38
C6 WP-BC	4.76	5.64	5.64	5.36	4.17	3.73	2.89

concentrations are overpredicted and underpredicted, respectively, by the WP-BC method. The general performance of PM_{2.5} forecasts is enhanced by the WP-BC method, especially at the off-island stations. The very good performance of the WP-BC method in the off-island area may be due to a less complicated emission source contribution over the off-island area; as a result, the systematic underestimations can be successfully removed with the bias-correction method.

Fig. 8 presents the root mean square error (RMSE) of the PM_{2.5} forecasts at each surface station from the AQF system and the WP-BC method. The RMSE is averaged for the days within each cluster throughout the one-year evaluation period. Among the six clusters, the highest RMSEs of the AQF PM_{2.5} forecasts appear in the C3 cluster and occur at stations located in the central to southern parts of western Taiwan (CT, YCN and KP subregions), where the worst PM_{2.5} pollution is typically observed. The RMSE is higher in the KP subregion than in the other regions in clusters C1 and C2. The RMSE is lower in clusters C5 and C6 than in the other clusters. In C5, the RMSE is slightly higher in northern Taiwan, where the observed PM_{2.5} concentrations are also higher than those in other regions. The RMSE is significantly reduced by the WP-BC methods, and the improvements are the most significant in the CT, YCN and KP subregions in the C3 cluster.

3.3. Evaluation statistics

To assess the performance of the CMAQ PM_{2.5} forecasts and WP-BC method, the MB and RMSE, as defined in Yu et al. (2006), were

estimated. Table 3 presents the statistical scores from the daily mean CMAQ PM_{2.5} forecasts and WP-BC PM_{2.5} forecasts associated with each weather type.

From the observed mean PM_{2.5} concentrations, the highest concentrations occur in C3, followed by C2 and then C1. Systematic underprediction can be seen in all the WPs from the AQF PM_{2.5} forecasts, with the largest underprediction found in cluster C3. The PM_{2.5} underprediction is greatly reduced with the WP-BC method, as seen from the reduced MB and RMSE values. Overall, the RMSE of the WP-BC forecasts is lower than that of the AQF forecast for all classified weather types. The most significant improvement appears on days associated with a weak synoptic weather pattern (C3), where the RMSE is 11.45 ($\mu\text{g}/\text{m}^3$) with the AQF system and reduces to 8.22 ($\mu\text{g}/\text{m}^3$) with the WP-BC method. Compared with the raw model AQF system, the RMSE is reduced by approximately 30% with the WP-BC method.

To understand the AQF performance for the PM_{2.5} forecasts in different regions of Taiwan, Table 4 estimates the RMSE in seven subregions of Taiwan for each cluster. The performance of the AQF system tends to be the worst in the YCN and KP subregions, where the RMSE is higher than that in other regions. The highest RMSE (16.27 $\mu\text{g}/\text{m}^3$) occurs in the YCN subregion on days associated with a weak synoptic weather system (C3). The WP-BC method successfully reduces the RMSE of the PM_{2.5} forecasts compared to that of the AQF PM_{2.5} forecasts.

Fig. 9 further presents the RMSE values as a function of the observed daily mean PM_{2.5} concentrations for each cluster to examine the performance of PM_{2.5} forecasts in different concentration ranges. The AQF system shows the highest RMSE values in the high PM_{2.5} concentration ranges ($>35 \mu\text{g}/\text{m}^3$) in all the clusters except C5. When the observed PM_{2.5} concentrations are low ($<12 \mu\text{g}/\text{m}^3$), the WP-BC method is able to reduce the RMSE values in C5 and C6 compared to the RMSE of the AQF forecasts; however, the WP-BC method results in wider variations in the RMSE than do the AQF forecasts in clusters C1–C4, with the highest RMSE appearing in C3. The degraded performance of the WP-BC method is attributed to a linear-regression assumption used for bias correction. For PM_{2.5} concentrations within 12–20 $\mu\text{g}/\text{m}^3$, in general, the WP-BC method performs better than the AQF system, except in cluster C3. For observed PM_{2.5} concentrations within 20–35 $\mu\text{g}/\text{m}^3$, the WP-BC method performs very well, with smaller RMSE values and narrower RMSE distributions. For high PM_{2.5} concentrations ($>35 \mu\text{g}/\text{m}^3$), the WP-BC method performs well except in clusters C5 and C6. The increased RMSE with the WP-BC method in clusters C5 and C6 is mainly due to the misclassified WP, which is discussed in the next section.

4. Discussion of the WP-BC method and its application in real-time AQF systems

The evaluations and assessments presented in Section 3 provide an overview of the performance of the WP-BC method. To understand the applicability of the WP-BC method in the real-time AQF system, the one-year training datasets from October 2018 to September 2019 are used to correct an independent period from October 2019 to May 2020. The number of occurrence days is 52, 64, 72, 24, 16, and 16 in clusters C1, C2, C3, C4, C5, and C6, respectively, during the period of October 2019 to May 2020. Fig. 10 presents the PM_{2.5} concentrations in a time-space variation from the surface observations, the AQF system, and the WP-BC method. The CMAQ model underpredicts the PM_{2.5} for low concentrations. The off-island stations presented systematic PM_{2.5} underpredictions from the AQF system. The general performance of the PM_{2.5} forecasts with the WP-BC method is enhanced.

Further estimation of the RMSE from the CMAQ and WP-BC PM_{2.5} forecasts for the period of October 2019 to May 2020 are presented in Fig. 11. Similar to Table 3, the statistical scores from the daily mean CMAQ PM_{2.5} forecasts and WP-BC PM_{2.5} forecasts from October 2019 to May 2020 in each cluster is summarized in Table S2. The assessment indicates that the WP-BC method is able to reduce the RMSE of PM_{2.5} forecasts compared to the RMSE of the CMAQ AQF system. This

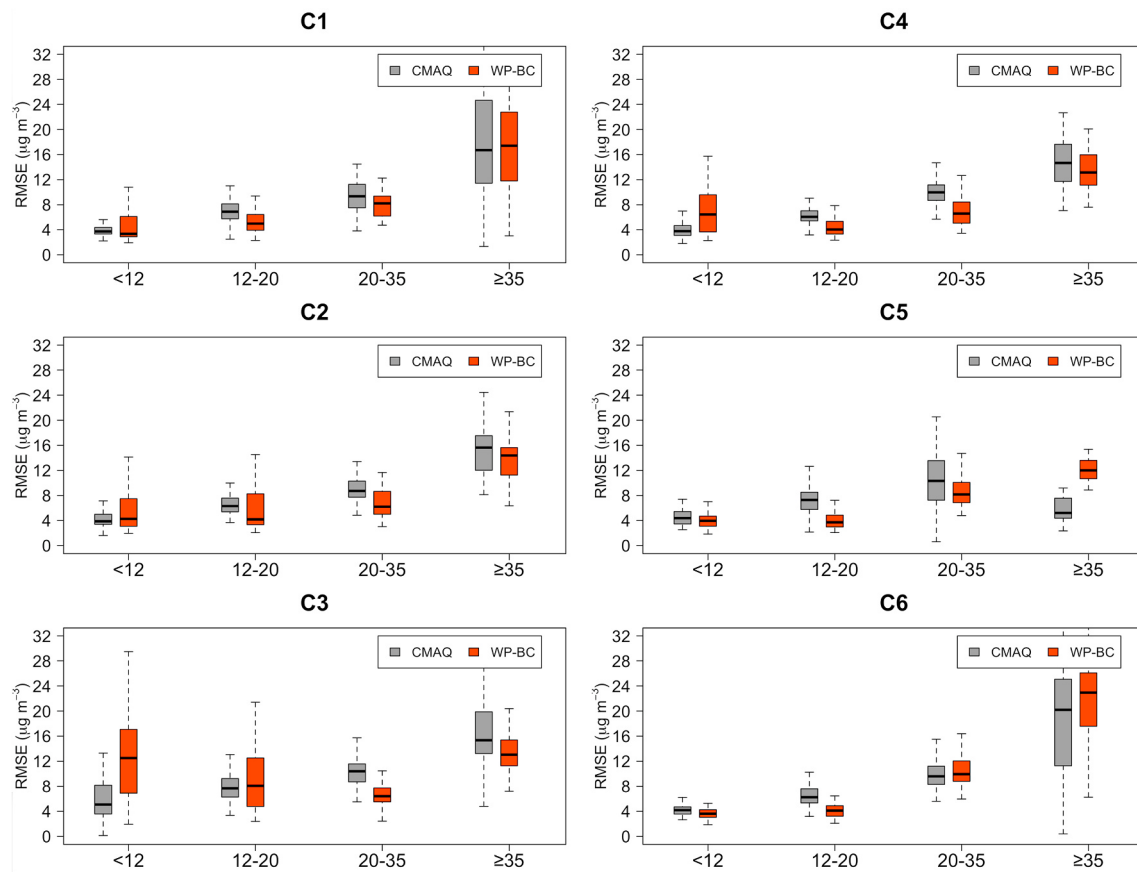


Fig. 9. RMSEs across the observed daily mean $\text{PM}_{2.5}$ concentration ranges from the AQF system $\text{PM}_{2.5}$ forecasts and WP-BC $\text{PM}_{2.5}$ forecasts.

evaluation proves the feasibility of applying the WP-BC method in a real-time AQF system in the future.

According to Hsu and Cheng (2016, 2019), the variation in the synoptic WP has a direct and significant impact on air pollution in Taiwan. In principle, the categorization of $\text{PM}_{2.5}$ biases into different WPs implies that errors can be associated with different circulation patterns. It is recognized that biases in different WPs are produced by different physical mechanisms, which can allow for a physically coherent correction. Moreover, different circulation patterns imply that the $\text{PM}_{2.5}$ originates from different emission sources, which can allow for a chemically coherent correction.

The separation of bias patterns into different WPs further reveals the deficiency of physical and chemical processes in the current AQF system, which leads to $\text{PM}_{2.5}$ biases. These processes should be improved in the future to enhance the raw model forecasting capability. For example, to enhance the $\text{PM}_{2.5}$ forecasting capability in the YCN subregion of cluster C3, updating the emission sources in the YCN subregion should be considered the top priority. In addition, overestimation of the wind speed leads to $\text{PM}_{2.5}$ underpredictions, which need to be addressed. Methods such as data assimilation can reduce the simulated wind speeds in the planetary boundary layer by assimilating near-surface observations (Wang et al., 2018).

The performance of the bias-correction method strongly relies on the accuracy of WP identification. In this study, six WPs were identified; however, there are weather types that do not fit into the six currently classified WPs and should be identified separately. For example, with the eastward movement of the East Asian anticyclone, a southeasterly wind prevails over Taiwan before the cold-front approaches, which can be mixed into the C3 type, and some days are misclassified as the C5 and C6 weather types. The days classified in clusters C5 and C6 with high $\text{PM}_{2.5}$ concentrations ($>35 \mu\text{g/m}^3$) were actually misclassified. The WPs

of those days are closer to the C3 WP instead of the C5 and C6 WPs. This explains why the WP-BC method does not perform well on the days associated with high $\text{PM}_{2.5}$ concentrations in clusters C5 and C6. Philipp et al. (2016) applied 33 classification methods to examine the agreement among different methods in classifying circulation patterns and concluded that a broad comparison of methods is required to find a suitable classification system. Different classification methods are currently being evaluated to enhance the WP classification accuracy; however, this is beyond the scope of the present study.

5. Conclusions

A real-time AQF system using the WRF meteorological model and CMAQ air quality model was developed in Taiwan and has been in operation since July 2015. The one-year CMAQ archived $\text{PM}_{2.5}$ forecasts (October 2018 to September 2019) were evaluated against surface air quality monitoring stations to assess the AQF capability. In addition, a bias-correction approach that accounts for information on synoptic weather types was developed to postprocess the AQF $\text{PM}_{2.5}$ forecasts.

The bias-correction method incorporates cluster-analysis-based synoptic WP classification and consists of the following steps: (1) determine the synoptic WPs using K-means cluster analysis (six WPs were identified); (2) estimate the $\text{PM}_{2.5}$ bias at each surface station using the archived historical AQF $\text{PM}_{2.5}$ forecasts; (3) categorize the $\text{PM}_{2.5}$ bias according to the six synoptic WPs; (4) develop a linear-regression relationship between the AQF $\text{PM}_{2.5}$ bias and $\text{PM}_{2.5}$ forecasts for the six WPs; and (5) postcorrect the $\text{PM}_{2.5}$ forecasts.

The WP determination follows Hsu and Cheng (2019); in total, six WPs were identified. The analysis of the MB associated with the six WPs reveals distinct bias distributions in different regions of Taiwan. The assessment of the one-year AQF $\text{PM}_{2.5}$ forecasts indicate an overall

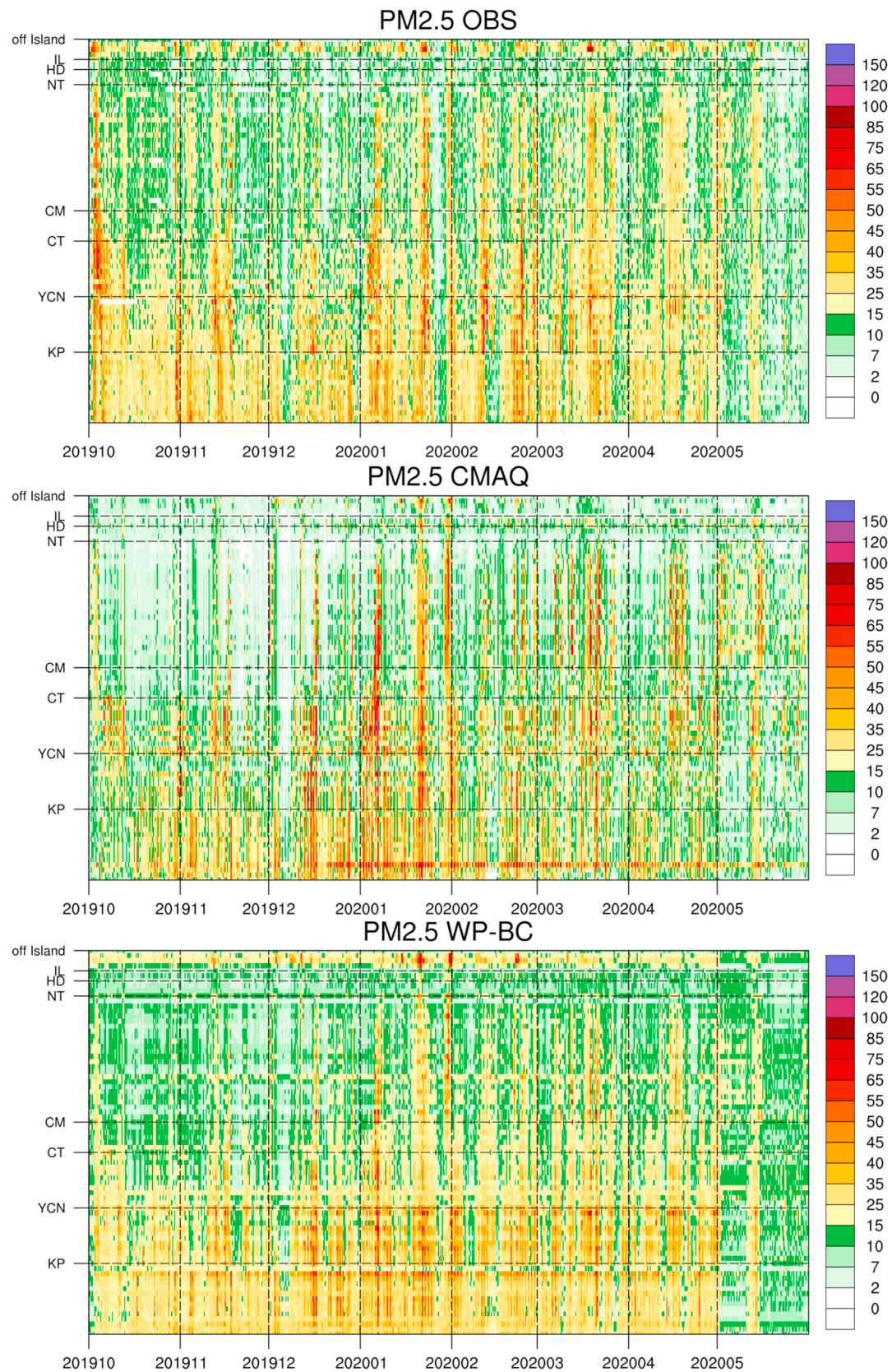


Fig. 10. Distributions of the PM_{2.5} concentrations ($\mu\text{g}/\text{m}^3$) in a time-space diagram from surface observations (top), the AQF system (middle), and the WP-BC (bottom) method. The horizontal axis is the time evolution. The vertical axis is sorted according to the station locations in the order of off-island, eastern Taiwan (IL, HD), NT, CM, CT, YCN, and KP subregions (from the upstream to the downstream areas).

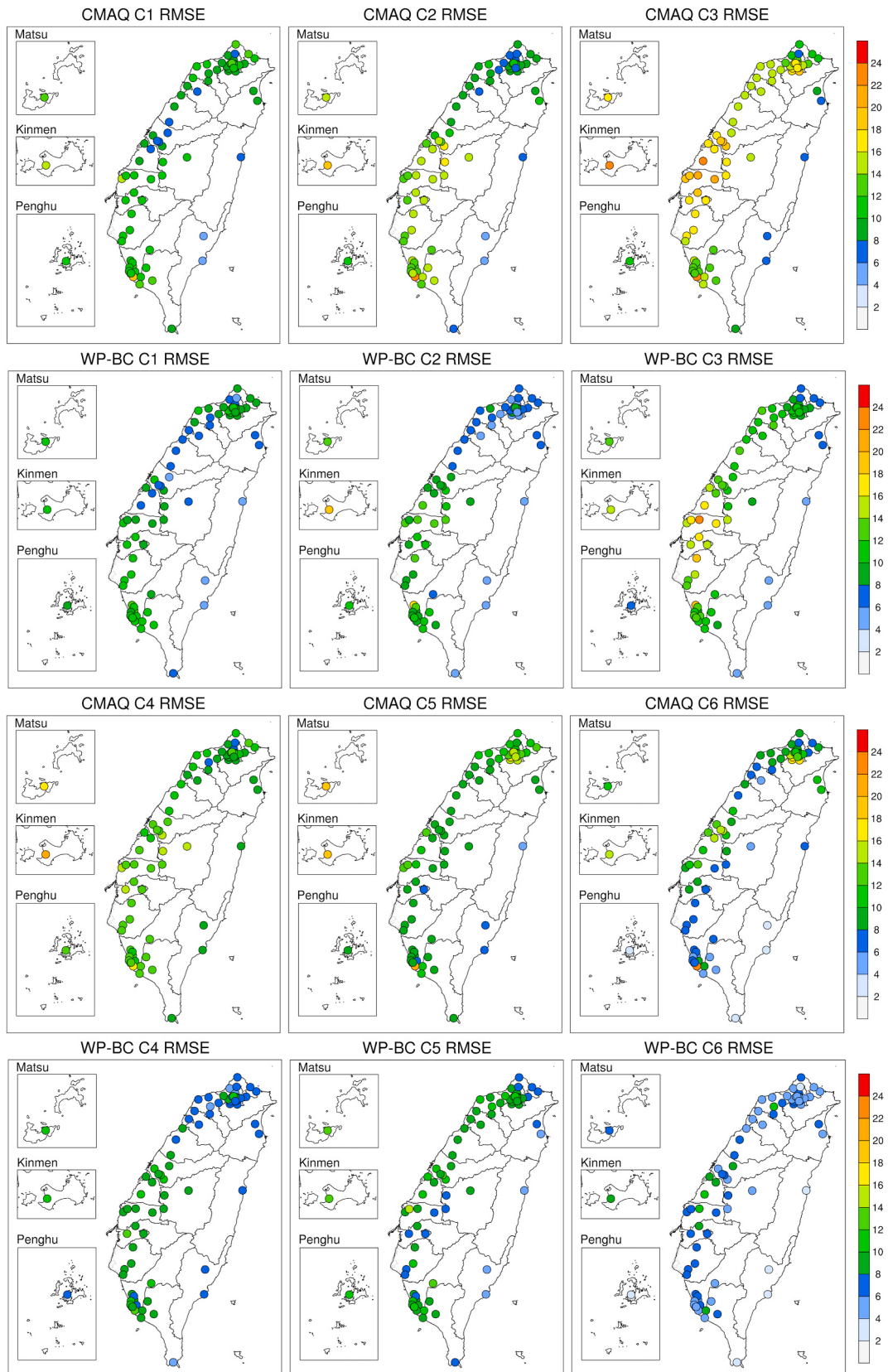


Fig. 11. RMSEs of $\text{PM}_{2.5}$ forecasts ($\mu\text{g}/\text{m}^3$) averaged from October 2019 to May 2020 at surface stations associated with six WPs. First and second row from the top is RMSEs in clusters C1 to C3 with the AQF system and WP-BC method, respectively. Third and fourth row from the top is RMSEs in clusters C4 to C6 with the AQF system and WP-BC method, respectively.

underprediction in most areas of Taiwan; in particular, consistent underpredictions are obtained at the off-island stations throughout the one-year evaluation period. The YCN subregion also exhibits consistent PM_{2.5} underpredictions in all the clusters, and serious underprediction is seen on the days associated with weak synoptic weather conditions (C3), for which a severe PM_{2.5} event is likely to occur in Taiwan. This serious bias can prevent air quality forecasters from publishing accurate daily air quality conditions. Fortunately, the bias-correction method proposed in this study is able to reduce the PM_{2.5} forecasting error and enhance the PM_{2.5} forecasting capability.

The WP-BC method significantly reduces the AQF PM_{2.5} errors and evaluations of the statistical performance (RMSE and MB) proved its effectiveness at correcting the AQF PM_{2.5} bias. The improvement is most significant at the off-island stations and in the YCN subregion. The overall RMSE is lower with the WP-BC method than with the AQF system; however, the performance of the former degrades at low PM_{2.5} concentrations due to a linear-regression assumption, for which the PM_{2.5} bias is assumed to vary linearly with the AQF PM_{2.5} forecast bias.

The characteristics of the AQF PM_{2.5} biases are distinct in different regions of Taiwan. Further separation into different synoptic WPs increases the understanding of the possible physical and chemical processes leading to the PM_{2.5} biases, which is beneficial for enhancing the AQF capability in the future.

The build-up of the linear-regression relationship using the year-long data (October 2018 to September 2019) successfully reduced the RMSE of the eight-month PM_{2.5} forecasts (October 2019 to May 2020). This indicates that the WP-BC methodology can be adopted easily for correcting the PM_{2.5} forecasts in a real-time AQF system. We are in the process of integrating the synoptic weather type classification method into the real-time AQF system. The forecasting output from the AQF system together with the past five years of observation datasets is used as input for the K-means clustering method. The WP-dependent training data should contain at least a one-year data period to include the complete seasonal variation. Moreover, due to variations in anthropogenic emissions (e.g., mitigation strategies), the WP-dependent training dataset and the linear-regression relationship should be rebuilt from time to time. Updating the methodology every year should be beneficial for the real-time AQF system. We are confident that the application of the WP-BC method in a real-time AQF system can enhance the daily PM_{2.5} forecasts effectively. Last, with better distinctions among the synoptic WP classifications, the performance of the WP-BC method can be further enhanced.

Data availability

The ERA5 dataset can be downloaded from the European Centre for Medium-Range Weather Forecasts (ECMWF) web page (<https://www.ecmwf.int/en/forecasts/datasets/reanalysis-datasets/era5>). The PM_{2.5} observation data, AQF PM_{2.5} forecasts and WP-BC PM_{2.5} forecasts consist of hourly outputs at surface air quality stations, have been uploaded to the journal website.

CRediT authorship contribution statement

Fang-Yi Cheng: Investigation, Writing - review & editing, Conceptualization, Supervision. **Chih-Yung Feng:** Methodology. **Zhih-Min Yang:** Software, Data curation. **Chia-Hua Hsu:** Software. **Ka-Wa Chan:** Methodology. **Chia-Ying Lee:** Visualization, Validation. **Shuenn-Chin Chang:** Data curation, Resources.

Declaration of competing interest

The authors declare that they have no known competing financial interests or personal relationships that could have appeared to influence the work reported in this paper.

Acknowledgments

This work was supported by a TWEPA grant [EPA-107-FALL-03-A140]. The contents are solely the responsibility of the grantee and do not always represent the official views of the TWEPA. We thank the Central Weather Bureau and TWEPA for providing the surface station datasets.

Appendix A. Supplementary data

Supplementary data to this article can be found online at <https://doi.org/10.1016/j.atmosenv.2020.117909>.

Funding

This work was supported by a TWEPA grant [EPA-107-FALL-03-A140].

Role of the funding source

The funding source had no involvement.

References

- Appel, K.W., Napelenok, S.L., Foley, K.M., Pye, H.O.T., Hogrefe, C., Luecken, D.J., Bash, J.O., Roselle, S.J., Pleim, J.E., Foroutan, H., Hutzell, W.T., Pouliot, G.A., Sarwar, G., Fahey, K.M., Gantt, B., Gilliam, R.C., Kang, D., Mathur, R., Schwede, D.B., Spero, T.L., Wong, D.C., Young, J.O., 2017. Description and evaluation of the Community Multiscale Air Quality (CMAQ) modeling system version 5.1. *Geosci. Model Dev. (GMD)* 10, 1703–1732.
- Bárdossy, A., Pegram, G., 2011. Downscaling precipitation using regional climate models and circulation patterns toward hydrology. *Water Resour. Res.* 47, W04505.
- Businger, J., Wyngaard, J., Izumi, Y., Bradley, E., 1971. Flux-profile relationships in atmospheric surface layer. *J. Atmos. Sci.* 28 (2), 181–189.
- Byun, D.W., Ching, J.K.S., 1999. Science Algorithms of the EPA Models-3 Community Multiscale Air Quality (CMAQ) Modeling System. *EPA/600/R-99/030*. USEPA, Research Triangle Park, NC, USA.
- Byun, D., Schere, K.L., 2006. Review of the governing equations, computational algorithms, and other components of the models-3 Community Multiscale Air Quality (CMAQ) modeling system. *Appl. Mech. Rev.* 59, 51–77.
- Byun, D.W., Young, J., Pleim, J., Odman, M.T., Alapati, K., 1999. Numerical transport algorithms for the community Multiscale Air quality (CMAQ) chemical transport model in generalized coordinates. *EPA/600/R-99/030*. In: Byun, D.W., Ching, J.K.S. (Eds.), *Science Algorithms of the EPA Models-3 Community Multiscale Air Quality (CMAQ) Modeling System*. NERL, Research Triangle Park, NC.
- Chen, T.-F., Tsai, C.-Y., Chang, K.-H., 2013. Performance evaluation of atmospheric particulate matter modeling for East Asia. *Atmos. Environ.* 77, 365–375.
- Cheng, F.Y., Chen, Y., 2018. Variations in soil moisture and their impact on land-air interactions during a 6-month drought period in Taiwan. *Geoscience Letters* 5 (26), 1–14.
- Cheng, F.Y., Hsu, C.H., 2019. Long-term variations in PM_{2.5} concentrations under changing meteorological conditions in Taiwan. *Sci. Rep.* 9, 6635.
- Cheng, F.Y., Chin, S.C., Liu, T.H., 2012. The role of boundary layer schemes in meteorological and air quality simulations of the Taiwan area. *Atmos. Environ.* 54, 714–727.
- Cheng, F.Y., Hsu, Y.C., Lin, P.L., Lin, T.H., 2013. Investigation of the effects of different land use and land cover patterns on mesoscale meteorological simulations in the Taiwan area. *Journal of Applied Meteorology and Climatology* 52, 570–587.
- Cheng, F.Y., Lin, C.F., Wang, Y.T., Tsai, J.L., Tsuang, B.J., Lin, C.H., 2019. Impact of effective roughness length on mesoscale meteorological simulations over heterogeneous land surfaces in Taiwan. *Atmosphere* 10, 805.
- De Ridder, K., Kumar, U., Lauwaet, D., Blyth, L., Lefebvre, W., 2012. Kalman filter-based air quality forecast adjustment. *Atmos. Environ.* 50, 381–384.
- Delle Monache, L., Nipen, T., Deng, X., Zhou, Y., Stull, R., 2006. Ozone ensemble forecasts: 2. A Kalman filter predictor bias correction. *J. Geophys. Res.* 111, D05308.
- Delle Monache, L., Djalalova, I., Wilczak, J., 2014. Analog-based postprocessing methods for air quality forecasting. In: Steyn, D.G., Rao, S.T. (Eds.), *Air Pollution Modeling and its Application XXXIII*. Springer, Berlin/Heidelberg, Germany, pp. 237–239.
- Djalalova, I., Delle Monache, L., Wilczak, J., 2015. PM_{2.5} analog forecast and Kalman filter post-processing for the Community Multiscale Air Quality (CMAQ) model. *Atmos. Environ.* 108, 76–87.
- Ghim, Y.S., Choi, Y., Kim, S., Bae, C.H., Park, J., Shin, H.J., 2017. Evaluation of model performance for forecasting fine particle concentrations in Korea. *Aerosol and Air Quality Research* 17, 1856–1864.
- Gilliam, R.C., Hogrefe, C., Godowitch, J.M., Napelenok, S., Mathur, R., Rao, S.T., 2015. Impact of inherent meteorology uncertainty on air quality model predictions. *J. Geophys. Res.: Atmosphere* 120, 12259–12280.
- Gómez-Navarro, J.J., Raible, C.C., Bozhinova, D., Martius, O., García Valero, J.A., Montávez, J.P., 2018. A new region-aware bias-correction method for simulated

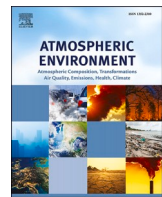
- precipitation in areas of complex orography. *Geosci. Model Dev. (GMD)* 11, 2231–2247.
- Guenther, A.B., Jiang, X., Heald, C.L., Sakulyanontvittaya, T., Duhl, T., Emmons, L.K., Wang, X., 2012. The model of emissions of gases and aerosols from nature version 2.1 (MEGAN2.1): an extended and updated framework for modeling biogenic emissions. *Geosci. Model Dev. (GMD)* 5, 1471–1492.
- Hersbach, H., Dee, D., 2016. ERA5 reanalysis is in production. *ECMWF Newsletter* 147, 7.
- Holnicki, P., Nahorski, Z., 2015. Emission data uncertainty in urban air quality modeling—case study. *Environ. Model. Assess.* 20, 583–597.
- Holtslag, A.A.M., Svensson, G., Baas, P., Basu, S., Beare, B., Beljaars, A.C.M., Bosveld, F.C., Cuxart, J., Lindvall, J., Steeneveld, G.J., Tjernström, M., 2013. Stable atmospheric boundary layers and diurnal cycles—challenges for weather and climate models. *Bull. Am. Meteorol. Soc.* 94, 1691–1706.
- Hori, M.E., Ueda, H., 2006. Impact of global warming on the East Asian winter monsoon as revealed by nine coupled atmosphere-ocean GCMs. *Geophys. Res. Lett.* 33, L03713.
- Hsu, C.-H., Cheng, F.-Y., 2016. Classification of weather patterns to study the influence of meteorological characteristics on PM_{2.5} concentrations in Yunlin County, Taiwan. *Atmos. Environ.* 144, 397–408.
- Hsu, C.H., Cheng, F.Y., 2019. Synoptic weather patterns and associated air pollution in Taiwan. *Aerosol and Air Quality Research* 19, 1139–1151.
- Hsu, C.H., Cheng, F.Y., Chang, H.Y., Lin, N.H., 2019. Implementation of a dynamical NH3 emissions parameterization in CMAQ for improving PM_{2.5} simulation in Taiwan. *Atmos. Environ.* 218, 116923.
- Huang, J., McQueen, J., Wilczak, J., Djalalova, I., Stajner, I., Shafran, P., Allured, D., Lee, P., Pan, L., Tong, D., Huang, H.C., DiMego, G., Upadhyay, S., Delle Monache, L., 2017. Improving NOAA NAQFC PM_{2.5} predictions with a bias correction approach. *Weather Forecast.* 32, 407–421.
- Hung, H.M., Hoffmann, M.R., 2015. Oxidation of gas-phase SO₂ on the surfaces of acidic microdroplets: implications for sulfate and sulfate radical anion formation in the atmospheric liquid phase. *Environ. Sci. Technol.* 49, 13768–13776.
- Kang, D., Mathur, R., Trivikrama Rao, S., Yu, S., 2008. Bias adjustment techniques for improving ozone air quality forecasts. *J. Geophys. Res.* 113, D23308.
- Kang, D., Mathur, R., Trivikrama Rao, S., 2010a. Assessment of bias-adjusted PM_{2.5} air quality forecasts over the continental United States during 2007. *Geosci. Model Dev. (GMD)* 3, 309–320.
- Kang, D., Mathur, R., Trivikrama Rao, S., 2010b. Real-time bias-adjusted O₃ and PM_{2.5} air quality index forecasts and their performance evaluations over the continental United States. *Atmos. Environ.* 44, 2203–2212.
- Kohonen, T., 2001. Self-organizing Maps. Ser. Information Sciences, vol. 30. Springer, Berlin.
- Lai, H.C., Lin, M.C., 2020. Characteristics of the upstream flow patterns during PM_{2.5} pollution events over a complex island topography. *Atmos. Environ.* 227, 117418.
- Lee, P., McQueen, J., Stajner, I., Huang, J., Pan, L., Tong, D., Kim, H., Tang, Y., Kondragunta, S., Ruminski, M., Lu, S., Rogers, E., Saylor, R., Shafran, P., Huang, H.C., Gorline, J., Upadhyay, S., Artz, R., 2017. NAQFC developmental forecast guidance for fine particulate matter (PM_{2.5}). *Weather Forecast.* 32, 343–360.
- Lee, M., Lin, L., Chen, C.Y., Tsao, Y., Yao, T.H., Fei, M.H., Fang, S.H., 2020. Forecasting air quality in Taiwan by using machine learning. *Sci. Rep.* 10, 4153.
- Li, M., Zhang, Q., Kurokawa, J.-I., Woo, J.-H., He, K., Lu, Z., Ohara, T., Song, Y., Streets, D.G., Carmichael, G.R., Cheng, Y., Hong, C., Huo, H., Jiang, X., Kang, S., Liu, F., Su, H., Zheng, B., 2017. MIX: a mosaic Asian anthropogenic emission inventory under the international collaboration framework of the MICS-Asia and HTAP. *Atmos. Chem. Phys.* 17, 935–963.
- Li, J., Sharma, A., Evans, J., Johnson, F., 2018. Addressing the mischaracterization of extreme rainfall in regional climate model simulations—a synoptic pattern based bias-correction approach. *J. Hydrol.* 556, 901–912.
- Lyu, B.L., Zhang, Y.H., Hu, Y.T., 2017. Improving PM_{2.5} air quality model forecasts in China using a bias-correction framework. *Atmosphere* 8, 147.
- MacQueen, J.B., 1967. Some methods for classification and analysis of multivariate observations. In: Proceedings of the Fifth Berkeley Symposium on Mathematical Statistics and Probability. University of California Press, Berkeley, CA.
- Mathur, R., Yu, S., Kang, D., Schere, K.L., 2008. Assessment of the wintertime performance of developmental particulate matter forecasts with the Eta-Community Multiscale Air Quality modeling system. *J. Geophys. Res.* 113, D02303.
- McNider, R.T., Pour-Bazar, A., 2020. Meteorological modeling relevant to mesoscale and regional air quality applications: a review. *J. Air Waste Manag. Assoc.* 70, 2–43.
- Murphy, B.N., Woody, M.C., Jimenez, J.L., Carlton, A.M.G., Hayes, P.L., Liu, S., Ng, N.L., Russell, L.M., Setyan, A., Xu, L., Young, J., Zaveri, R.A., Zhang, Q., Pye, H.O.T., 2017. Semivolatile POA and parameterized total combustion SOA in CMAQv5.2: impacts on source strength and partitioning. *Atmos. Chem. Phys.* 17, 11107–11133.
- Otte, T.L., Pouliot, G., Pleim, J.E., Young, J.O., Schere, K.L., Wong, D.C., Lee, P.C.S., Tsidulko, M., McQueen, J.T., Davidson, P., Mathur, R., Chuang, H.Y., DiMego, G., Seaman, N.L., 2005. Linking the Eta model with the Community Multiscale Air Quality (CMAQ) modeling system to build a national air quality forecasting system. *Weather Forecast.* 20, 367–384.
- Philipp, A., Beck, C., Hüth, R., Jacobbeit, J., 2016. Development and comparison of circulation type classifications using the COST 733 dataset and software. *Int. J. Climatol.* 36 (7), 2673–2691.
- Photiadou, C., van den Hurk, B., van Delden, A., Weerts, A., 2016. Incorporating circulation statistics in bias correction of GCM ensembles: hydrological application for the Rhine basin. *Clim. Dynam.* 46, 187–203.
- Pleim, J.E., 2007. A combined local and nonlocal closure model for the atmospheric boundary layer. Part I: model description and testing. *Journal of Applied Meteorology and Climatology* 46, 1383–1395.
- Pye, H.O.T., Murphy, B.N., Xu, L., Ng, N.L., Carlton, A.G., Guo, H., Weber, R., Vasilakos, P., Appel, K.W., Budisulistiorini, S.H., Surratt, J.D., Nenes, A., Hu, W., Jimenez, J.L., Isaacman-VanWertz, G., Misztal, P.K., Goldstein, A.H., 2017. On the implications of aerosol liquid water and phase separation for organic aerosol mass. *Atmos. Chem. Phys.* 17, 343–369.
- Serafin, S., Adler, B., Cuxart, J., De Wekker, S., Gohm, A., Grisogono, B., Kalthoff, N., Kirshbaum, D., Rotach, M., Schmidli, J., Stiperski, I., Većenaj, Ž., Zardi, D., 2018. Exchange processes in the atmospheric boundary layer over mountainous terrain. *Atmosphere* 9, 102.
- Skamarock, W.C., Klemp, J.B., Dudhia, J., Gill, D.O., Barker, D.M., Duda, M.G., Huang, X.-Y., Wang, W., Powers, J.G., 2008. A Description of the Advanced Research WRF Version 3. National Center for Atmospheric Research Technical Note, NCAR, Boulder, CO, USA.
- Stajner, I., Davidson, P., Byun, D., McQueen, J., Draxler, R., Dickerson, P., Meagher, J., 2012. US national air quality forecast capability: expanding coverage to include particulate matter. In: Steyn, Douw G., Castelli, Silvia Trini (Eds.), NATO/ITM Air Pollution Modeling and its Application XXI. Springer, Netherlands, pp. 379–384. https://doi.org/10.1007/978-94-007-1359-8_64.
- Wang, L.-J., Hsu, C.-H., Cheng, F.-Y., Wang, S.-H., Yang, S.-C., 2018. Impact of Lidar Data on Planetary Boundary Layer Wind and PM_{2.5} Prediction in Taiwan. Short abstract, Asia Oceania Geosciences Society Annual Meeting, 2018, Hawaii, USA.
- Yarwood, G., Rao, S.T., Yocke, M., Whitten, G., 2005. Updates to the Carbon Bond Chemical Mechanism: CB05. Report to the U.S. Environmental Protection Agency, RT-0400675.
- Yu, S., Eder, B., Dennis, R., Chu, S.H., Schwartz, S.E., 2006. New unbiased symmetric metrics for evaluation of air quality models. *Atmos. Sci. Lett.* 7, 26–34.
- Žabkar, R., Honzák, L., Skok, G., Forkel, R., Rakovec, J., Ceglar, A., Žagar, N., 2015. Evaluation of the high resolution WRF-Chem (v3.4.1) air quality forecast and its comparison with statistical ozone predictions. *Geosci. Model Dev. (GMD)* 8, 2119–2137.
- Zhao, Y., Nielsen, C.P., Lei, Y., McElroy, M.B., Hao, J., 2011. Quantifying the uncertainties of a bottom-up emission inventory of anthropogenic atmospheric pollutants in China. *Atmos. Chem. Phys.* 11, 2295–2308.
- Zheng, B., Zhang, Q., Zhang, Y., He, K.B., Wang, K., Zheng, G.J., Duan, F.K., Ma, Y.L., Kimoto, T., 2015. Heterogeneous chemistry: a mechanism missing in current models to explain secondary inorganic aerosol formation during the January 2013 haze episode in North China. *Atmos. Chem. Phys.* 15, 2031–2049.

Update

Atmospheric Environment

Volume 254, Issue , 1 June 2021, Page

DOI: <https://doi.org/10.1016/j.atmosenv.2021.118263>



Corrigendum to “Evaluation of real-time PM_{2.5} forecasts with the WRF-CMAQ modeling system and weather-pattern-dependent bias-adjusted PM_{2.5} forecasts in Taiwan”

Fang-Yi Cheng ^{a,*}, Chih-Yung Feng ^b, Zhih-Min Yang ^b, Chia-Hua Hsu ^{a,c}, Ka-Wa Chan ^a, Chia-Ying Lee ^a, Shuenn-Chin Chang ^d

^a Department of Atmospheric Sciences, National Central University, Taiwan

^b Manysplendid Infotech, Taipei, Taiwan

^c Department of Mechanical Engineering, University of Colorado, Boulder, CO, USA

^d Environmental Protection Administration, Taipei, Taiwan

The format of Table 3 needs to be corrected, in particular the first column. Please refer to the following figure for the correct display of Table 3.

In addition, the MB should be shown in the first row of fifth column instead of M.

The authors would like to apologise for any inconvenience caused.

Cluster ^a	N ^a (days) ^a	obs_PM _{2.5} ^a ($\mu\text{g}/\text{m}^3$) ^a	PM _{2.5} forecast ^a ($\mu\text{g}/\text{m}^3$) ^a	MB ^a ($\mu\text{g}/\text{m}^3$) ^a	RMSE ^a ($\mu\text{g}/\text{m}^3$) ^a
C1 AQF ^a	42 ^a	17.43 ^a	14.22 ^a	-3.22 ^a	8.00 ^a
C1 WP ^a	- ^a	- ^a	17.52 ^a	0.09 ^a	6.20 ^a
C2 AQF ^a	64 ^a	19.46 ^a	16.63 ^a	-2.82 ^a	7.93 ^a
C2 WP ^a	- ^a	- ^a	19.47 ^a	0.02 ^a	5.95 ^a
C3 AQF ^a	75 ^a	25.44 ^a	21.05 ^a	-4.42 ^a	11.45 ^a
C3 WP ^a	- ^a	- ^a	25.51 ^a	0.10 ^a	8.22 ^a
C4 AQF ^a	57 ^a	17.13 ^a	13.48 ^a	-3.66 ^a	7.59 ^a
C4 WP ^a	- ^a	- ^a	17.20 ^a	0.07 ^a	5.40 ^a
C5 AQF ^a	32 ^a	12.84 ^a	10.15 ^a	-2.69 ^a	6.51 ^a
C5 WP ^a	- ^a	- ^a	12.78 ^a	-0.06 ^a	4.47 ^a
C6 AQF ^a	86 ^a	11.70 ^a	10.27 ^a	-1.42 ^a	6.10 ^a
C6 WP ^a	- ^a	- ^a	11.64 ^a	-0.05 ^a	4.87 ^a

DOI of original article: <https://doi.org/10.1016/j.atmosenv.2020.117909>.

* Corresponding author.

E-mail address: bonniecheng18@gmail.com (F.-Y. Cheng).